NATIONAL ADVISORY COMMITTEE FOR AERONAUTICS

2 DEC 1947

WARTIME REPORT

ORIGINALLY ISSUED
April 1945 as
Memorandum Report A5D04

CORRELATION OF WIND-TUNNEL PREDICTIONS WITH FLIGHT TESTS

OF A TWIN-ENGINE PATROL AIRPLANE. I - LONGITUDINAL-

STABILITY AND -CONTROL CHARACTERISTICS

By Noel K. Delany and William M. Kauffman

Ames Aeronautical Laboratory
Moffett Field, California

NACA

WASHINGTON

MR No. A5D04

NATIONAL ADVISORY COMMITTEE FOR AERONAUTICS

MEMORANDUM REPORT

for the

Bureau of Aeronautics, Navy Department

CORRELATION OF WIND-TUNNEL PREDICTIONS WITH FLIGHT TESTS

OF A TWIN-ENGINE PATROL AIRPLANE. I - LONGITUDINAL-

STABILITY AND -CONTROL CHARACTERISTICS

By Noel K. Delany and William M. Kauffman

SUMMARY

        The longitudinal-stability and -control characteristics
of a twin-engine patrol airplane as predicted from the
results of wind-tunnel tests of a powered model and as
measured in flight are compared in this report. The accuracy
of the wind-tunnel predictions and the reasons for dis-
crepancies are analyzed and discussed.

        The predictions from wind-tunnel-test data were in good
agreement with flight-test results. The results show that
such predicted flying-qualities characteristics are suffi-
ciently accurate to indicate the unsatisfactory longitudinal-
stability and -control characteristics of airplanes in the
preliminary design stage. The wind-tunnel data may be used
to deduce the chief reasons for these unsatisfactory charac-
teristics and to indicate possible methods of improvement.

        The aerodynamic longitudinal-stability derivatives as
estimated from flight-test data and as measured in the wind
tunnel were, in general, in good agreement. The differences
which occurred could be attributed partially to small
physical dissimilarities between the model and the airplane
and to inaccuracies involved in estimating the flight thrust
coefficients for use in matching power conditions.

INTRODUCTION

During the past several years the flying qualities of various airplanes have been estimated from the results of wind-tunnel tests made while the airplane was in the design stage. These predicted flying qualities have been used to determine compliance with the critical stability and control requirements. Basic changes to the airplane, necessary for correction of unsatisfactory characteristics, have been determined from these data. No comprehensive study of the accuracy of such methods of predictions has been made in the past, and it was considered desirable to compare in a detailed manner the predicted flying qualities with those measured in flight. Such a comparison should lead to a better understanding of the accuracy of the predictions and control characteristics, as well as to improvements in tests and methods which will result in more accurate estimates in the future.

As a part of this correlation program, flight tests were made to determine the flying qualities of a twin-engine airplane for the purpose of comparison with the results of tests of a 1/9-scale powered model in the Ames 7- by 10-foot wind tunnel (reference 1). Comparison of the test airplane with the wind-tunnel model indicated that the airfoil section of the model horizontal tail surface differed considerably from that on the actual airplane. Hence, the wind-tunnel-test results presented in reference 1 were not considered suitable for comparison with the flight-test results, and repeat tests were made with the model altered to correspond to the airplane. The predictions presented herein were computed from the results of these latter tests.

The longitudinal-stability and -control characteristics which are usually predicted from the wind-tunnel-stability and -control test data are static longitudinal stability, elevator control in maneuvering flight, and elevator control in landing. The results presented are confined to these characteristics, as they are critical in design work and are the longitudinal characteristics most suitable for comparison with flight-test data. The correlation of the lateral- and directional-stability and -control characteristics will be presented in a future report.

The stability and control characteristics as determined in flight and as predicted from the results of wind-tunnel

tests can be analyzed in various ways. In this report the
data derived from the wind-tunnel tests are first compared
with flight-test results in the form normally used in flight
reports (airspeeds, control forces, and elevator angles).
Comparisons of this type indicate the degree to which the
handling characteristics can be predicted, but do not readily
show the reasons for discrepancies. Hence, data in coef-
ficient form are derived from the static-longitudinal-
stability flight tests and compared in this form with the basic
wind-tunnel data. By this method the reasons for any disagree-
ment in the results can be determined in terms of basic aero-
dynamic coefficients and derivatives.

DESCRIPTION OF THE AIRPLANE

The airplane is a twin-engine, low-wing, medium-size
monoplane. It is equipped with retractable conventional-
type landing gear, twin vertical tail surfaces, and Fowler-
type wing flaps. Figures 1(a) and 1(b) are photographs of
the airplane as instrumented for the flight tests, and
figure 2 is a three-view drawing. The general specifications
and dimensions are presented in tables I, II, and III.

The de-icer boots and attaching rivnuts on the leading
edges of the wing and fixed tail surfaces were removed before
the flight tests in order to simulate conditions of the wind-
tunnel tests. The holes for the rivnuts were sealed with
scotch tape, and the airfoil leading edge was sanded smooth
(figs. 3 and 4).

The relation between control-column position and elevator
angle as measured on the ground with no load on the control
surface is given in figure 5. The elevator angle is defined
as the angle between the elevator and stabilizer chord lines.
The center section of the elevator consisted of an upper-
surface tail flap which operated only when the elevator was
at an up deflection (figs. 6 and 7). Motion of this tail flap
was resisted by a light bungee.

The force characteristics of the elevator system, which
was mass-unbalanced, as measured on the ground during slow
movements of the control column, are given in figure 8. The
elevator was equipped with combination trim and boost tabs.
The boost-tab ratio used during the flight tests was

approximately that recommended in reference 2. The relations between tab angle, tab cockpit-indicator setting, and elevator angle are shown in figure 9.

DESCRIPTION OF THE MODEL

The 1/9-scale model of the airplane (fig. 10) was the same model as used in reference 1 with the exception of the horizontal tail. The ordinates of the airfoil sections of the stabilizer and elevator were determined on the airplane at four stations. The contour of the model tail was then modified to correspond to the full-scale horizontal tail. The major differences between the model and the full-scale airplane were the lack of tabs on the model control surfaces and the method of fastening the elevator flap to the tail. On the airplane the elevator flap had a piano hinge; on the model it was attached to the elevators for up deflections, and to the tail cone for down deflections. There was a small gap between the stabilizer and elevator flap for up deflection of the elevators to eliminate friction effects in the measurement of the elevator hinge moments. The hinge moments were measured by means of resistance-type strain gages on the elevators. Power was supplied by two electric motors which drove two three-blade right-hand-rotation 1/9-scale propellers. The propeller-blade angle (30° at the 0.75 radius section) was selected as a good compromise between the high-and low-speed power-on flight conditions.

SYMBOLS

Definitions of abbreviations and symbols used in this report are as follows:

M.A.C.   wing mean aerodynamic chord, feet

V_i correct indicated airspeed, miles per hour

δ_e elevator angle, degrees (measured between elevator and stabilizer chord lines)

δ_T total elevator-tab angle, degrees (sum of trim and boost angles)

δ_t elevator trim-tab setting, degrees (does not include boost angle)

W airplane weight, pounds

A_Z the algebraic sum of the components along the airplane Z-axis, of the airplane acceleration and the acceleration due to gravity, in terms of the standard gravitational unit (32.2 ft/sec^2). Positive when directed upward.

q free-stream dynamic pressure, pounds per square foot

S wing area, square feet

C_L airplane lift coefficient (WA_Z/qS)

F_e elevator control force, pounds

T_c propeller thrust coefficient ($T/\rho V^2 D^2$)

i_T angle of incidence of the horizontal tail as measured from the fuselage reference line, degrees

x distance from leading edge of mean aerodynamic chord to test center-of-gravity location, foot per M.A.C. in feet

C_m pitching-moment coefficient about the center of gravity

$C_{m_{0.298}}$ pitching-moment coefficient about 0.298 M.A.C. $[C_L(x-0.298)]$

C_{m_δ} rate of change of pitching-moment coefficient with elevator angle $\partial C_m/\partial \delta_e$ (tab zero, lift coefficient constant)

$C_{m_{C_L}}$ rate of change of pitching-moment coefficient with lift coefficient $\partial C_m/\partial C_L$ (tab zero, elevator angle constant)

$C_{m_{i_T}}$ rate of change of pitching-moment coefficient with tail angle of incidence $\partial C_m/\partial i_T$ (tab zero, lift coefficient and elevator angle constant)

C_h elevator hinge-moment coefficient

C_{h_δ} rate of change of elevator hinge-moment coefficient with elevator angle $\partial C_h/\partial \delta_e$ (tab zero, lift coefficient constant)

$C_{h_{C_L}}$ rate of change of elevator hinge-moment coefficient with lift coefficient $\partial C_h/\partial C_L$ (tab zero, elevator angle constant)

$C_{h_{\delta_T}}$ rate of change of elevator hinge-moment coefficient with total tab angle $\partial C_h/\partial \delta_T$ (elevator angle and lift coefficient constant)

TESTS

As mentioned in the introduction, the results presented and discussed in this report are confined to the static longitudinal stability and control, elevator control in turning flight, and elevator control in landing. The following is a brief description of the tests and methods of computation.

Flight Tests

A description of the basic configurations for which flight tests were conducted is as follows:

Condition	Position			Power			Approximate indicated stalling airspeed (mph)
	Flap	Gear	Cowl flap	Manifold pressure (in.Hg)	Engine speed setting (rpm)	Brake horse-power per engine[1]	
Glide	Up	Up	Closed	Throttled	Propeller set in high pitch	— —	106
Climb	Up	Up	Closed	36	2400	1350	84
Landing	Full down (38°)	Down	Closed	Throttled	2400	— —	97
Approach	Full down (38°)	Down	Closed	20	2400	530	85

[1] From engine-performance chart for low-blower gear ratio at 6,000 feet.
Placard limit indicated airspeed — 350 miles per hour with flaps and gear up, 140 miles per hour with flaps and gear down.

Although there were small variations in weight due to
ballast and to fuel consumption, the average airplane gross
weight for all the tests was of the order of 26,500 pounds
(the normal airplane gross weight). This value has been used
as standard for computations. Three different center-of-
gravity locations were used during the tests (approx. 0.240,
0.275, and 0.325 M.A.C., flaps and gear up). Average test
values are noted on the figures. The average pressure alti-
tude for the static-longitudinal-stability and turning-flight
tests was 6000 feet.

Static-longitudinal-stability characteristics.- The
variation of elevator angle and control force with elevator-
tab setting was measured in steady straight unyawed flight
at various constant indicated airspeeds in the glide, climb,
landing, and approach conditions. At each airspeed the
pilot varied the tab setting to give about five different
values of control force over a sizable range. These tests
were performed while the center of gravity was at three
different locations. Cross plots of elevator angle and
control force as functions of indicated airspeed were
derived for various constant elevator trim-tab settings.

The pitching-moment characteristics of the airplane
were derived for the glide, climb, landing, and approach
conditions in the form of pitching-moment coefficient
$C_{m_{0.298}}$ as a function of lift coefficient C_L for various
constant elevator angles δ_e. In the determination of the
flight-test values, the variation of elevator angle
(corrected to total tab angle of zero) with lift coefficient
for each center-of-gravity location and flight condition
was obtained from replots of the curves of elevator angle
plotted against airspeed. The pitching-moment characteristics
for each condition were determined from cross plots (elevator
angle constant) of these curves. Lift and pitching-moment
coefficients were computed from the following formulas:

$$C_L = \frac{WA_Z}{qS}$$

$$C_{m_{0.298}} = -C_L(x - 0.298)$$

The elevator hinge-moment characteristics were derived for the glide, climb, landing, and approach conditions in the form of curves of elevator hinge-moment coefficient C_h as a function of lift coefficient C_L for constant elevator angles δ_e (total elevator tab angle of zero). It was not possible, despite the extensiveness of the test data, to use a direct analytical method to determine these elevator hinge-moment coefficients for flight. Small errors in the measurement of absolute values of elevator-tab setting were present from flight to flight, although the measured changes in elevator-tab setting for a given flight are considered accurate to $\pm 0.2^\circ$. Due to the large tab effectiveness, these small errors resulted in inconsistent data when an attempt was made to establish hinge-moment characteristics by a direct system of cross-plotting. In order to avoid this difficulty, a cut-and-try system was employed. The hinge-moment curves were estimated and adjusted to give characteristics which, when used in computations, resulted in the best agreement with the flight variations of control force with indicated airspeed.

Flight values of tab effectiveness $C_{h_{\delta_T}}$ (where δ_T = total tab angle) were determined from the slope, over the range of approximate linearity, of curves of elevator control force plotted against elevator trim-tab setting.

Elevator control in turning flight.- Steady turns of different constant acceleration factors were performed at various airspeeds in the climb conditions for three center-of-gravity locations. The variations of elevator-angle and control-force gradients $\Delta\delta_e/\Delta A_z$ and $\Delta F_e/\Delta A_z$ with airspeed were derived from these data.

Elevator control in landing.- Landings were made at different contact airspeeds over a safe and feasible range for the forward and rearward test center-of-gravity locations. These tests were performed in the flaps-full-down, power-off condition; that is, the landing condition used in the stability tests. The elevator-tab setting used during the landing tests was that normally used by the pilot in landings for the given test center-of-gravity location.

Wind-Tunnel Tests

The procedure for the wind-tunnel tests was the same as that outlined in reference 1, but the data presented herein

were obtained from repeat tests which have not been reported previously.

Basic data.- The data were obtained from constant-thrust-coefficient polar tests as described in reference 1. Conditions for the repeat tests are shown in the following table:

Model configuration	Elevator angle (deg)	Tail incidence (deg)	Thrust-coefficient range
Flaps and gear up	0, ±7	0	-0.04 to 0.6
Flaps and gear up	-15, -22, -28, -35	0	0 to 0.1
Flaps and gear up	0	3.75	0
Flaps 38°, gear down	0, ±7	0	-0.04 to 1.2
Flaps 38°, gear down	-15, -20	0	-0.04 to 0.3
Flaps 38°, gear down	0	3.75	0

Estimated flight $T_c - C_L$ relationships for the various power conditions (glide, climb, landing, and approach) were used in the derivations of cross plots for the various flight conditions. From these cross plots the wind-tunnel data of pitching-moment coefficient C_m and elevator hinge-moment coefficient C_h were obtained as a function of lift coefficient C_L. All data were corrected for wind-tunnel-wall effects and support-strut interference.

Methods for Predicting Stability and Control Characteristics

The variation of elevator angle and control force with indicated airspeed for steady straight unyawed flight and the variations of $\Delta F_e/\Delta A_Z$ and $\Delta\delta_0/\Delta A_Z$ in turning flight with indicated airspeed were computed by the methods outlined in

reference 3. The elevator-tab effectiveness used in the com-
putations was estimated from reference 4, as the model was not
equipped with tabs. In all of the computations the airplane
gross weight (26,500 lb), center-of-gravity locations (noted
on figs.), elevator mass unbalance, mechanical advantage of
the control system, and boost-tab ratio as measured on the air-
plane were used.

The variation of elevator angle and control force with
contact airspeed in landings was computed by the methods of
reference 3. The ground effects used in the computation of
the elevator angle and control force in landings were deter-
mined by two methods. Tests were made with a ground board in
the tunnel, and the effects of the ground on the upwash angle
at the wing and downwash at the tail were also computed from
reference 5.

RESULTS AND DISCUSSION

Static-Longitudinal-Stability Characteristics

The results for the various flight conditions are dis-
cussed first as to the degree of correlation (as indicated by
curves of the flight type) between flight-test and wind-tunnel
prediction. The reasons for the agreement or disagreement are
then explained by reference to the data in coefficient form.
For this analysis, examination of the static-longitudinal-
stability equations indicates that the differences between the
flight-test and predicted variations of elevator angle with
indicated airspeed can be ascribed to the following factors:

1. $\Delta C_{m_{C_L}}$ differences in $C_{m_{C_L}}$

2. ΔC_{m_δ} differences in C_{m_δ}

The stick-free stability characteristics in steady flight
can be shown by curves of C_h plotted against C_L. The
following equation can be written from these curves:

$$dC_h/dC_L = C_{h_{C_L}} + C_{h_\delta} (d\delta_e/dC_L)$$

The stick-free stability, as measured by the variation of
elevator stick force with indicated airspeed, is a function

of dC_h/dC_L, and hence differences between the flight-test and predicted variation of elevator control force with indicated airspeed can be ascribed to the following factors:

1. $\Delta(d\delta_e/dC_L)$ differences in stick-fixed stability, as measured by $d\delta_e/dC_L$

2. ΔC_{h_δ} differences in C_{h_δ}. The effect is largest when $d\delta_e/dC_L$ is large (forward c.g. location).

3. $\Delta C_{h_{C_L}}$ differences in $C_{h_{C_L}}$

The values of C_{h_δ} should include the balancing effect of the tab. However, for this airplane the wind-tunnel values of C_{h_δ}, either for tab neutral or with boost tab included, are in all cases greater than those measured in flight. For convenience the tab-neutral values of C_{h_δ} are used in the discussion, since the qualitative condition is the same for either condition. The value of tab effectiveness $C_{h_{\delta_T}}$ is presented in figure 11. It should be noted that the control force per unit of hinge-moment coefficient is a direct function of dynamic pressure, and hence a given change in hinge-moment coefficient can have a negligible effect on control force at low airspeeds but a large effect at high airspeeds.

Glide condition (figs. 12, 13, and 14).- Both the flight-test and predicted variation of elevator angle with indicated airspeed (fig. 12) show stick-fixed stability over the speed range for all test center-of-gravity locations. Compared to the flight-test stability, the predicted stability is slightly low in the low-speed range and slightly high in the high-speed range. Figure 13 indicates good agreement of values of C_{m_δ}, and analysis shows that the small differences in stability (as measured by $d\delta_e/dC_L$) are due primarily to the corresponding differences in $C_{m_{C_L}}$.

The stick-free stability (fig. 12) is positive in all cases. In the low-speed range with the center of gravity at 0.240 and 0.274 M.A.C., the predicted curves show greater stability (as measured by dF_e/dV_i) than flight. The predictions give less stability than flight in the low-speed range with the center of gravity at 0.323 M.A.C., and in the high-speed range for all test center-of-gravity locations. Figure 14 indicates that the wind-tunnel values of C_{h_δ} are more

negative than for flight, especially at up-elevator angles.
At the larger lift coefficients, the values of $C_{h_{C_L}}$ are in
good agreement, but at low lift coefficients the wind-tunnel
values are more negative. The greater stick-free stability
shown in figure 12 for the predicted curves in the low-airspeed
range with the center of gravity at 0.240 and 0.274 M.A.C. is
due primarily to the ΔC_{h_δ} effect, which is greater than the
destabilizing effect due to $\Delta(d\delta_e/dC_L)$. With the center of
gravity at 0.323 M.A.C., this destabilizing effect $\Delta(d\delta_e/dC_L)$
becomes predominant and causes lower predicted stability. In
the high-speed range (above trim) the predicted curves (fig.12)
are less stable for all center-of-gravity locations tested.
Here the destabilizing effects of $\Delta C_{h_{C_L}}$ and $\Delta(d\delta_e/dC_L)$ are
predominant, with the stabilizing effects of ΔC_{h_δ} becoming
smaller as the center of gravity moves rearward (0.323 M.AC.).

Climb condition (figs. 15, 16, and 17).- The predicted
elevator-angle curves (fig. 15) show stick-fixed stability,
except with the center of gravity at 0.324 M.A.C. Although
the agreement is good in the high-speed range, the flight
curves indicate instability in the low-speed range for all
test center-of-gravity locations. Examination of figure 16
shows that, since flight and wind-tunnel values of C_{n_δ} are
about the same, the higher predicted stability at large lift
coefficients is due primarily to the more negative values of
$C_{n_{C_L}}$ for the wind-tunnel tests.

The flight control-force curves presented in figure 15
for trim speeds of 145 miles per hour (approx. speed of best
climb) and 225 miles per hour (approx. level-flight speed)
indicate instability or unstable tendencies at low speeds in
all cases. The predicted curves show instability only for
0.324 M.A.C. center-of-gravity location, and, in general, show
greater stability at low speeds. At speeds above trim the only
instability occurs, both in flight and in predicted curves, for
the 0.324 M.A.C. location with 145 miles per hour trim speed.
In general, the predicted force curves indicate less stability
than flight for speeds above the trim speed. Figure 17 shows
that the wind-tunnel values of $C_{h_{C_L}}$ are slightly more nega-
tive at high and low values of lift coefficient, and that the
wind-tunnel values of C_{h_δ} are more negative than the flight
values throughout the lift-coefficient range. For both trim
conditions the same effects predominate in most cases. Below
the trim speeds, ΔC_{h_δ} effects are almost negligible because
$d\delta_e/dC_L$ is small, and the effect of $\Delta C_{h_{C_L}}$ is negligible.

However, the $\Delta(d\delta_e/dC_L)$ effect causes the wind-tunnel predictions to be more stable. Above the trim speeds the ΔC_{h_δ} and $\Delta(d\delta_e/dC_L)$ effects are negligible, but $\Delta C_{h_{C_L}}$ has a destabilizing effect.

Landing condition (figs. 18, 19, and 20).- The variation of elevator angle with airspeed (fig. 18) indicates large stick-fixed stability in all cases. The predicted stability agrees well with flight in the upper end of the test-speed range (about 140 mph), but is less than in flight in the low-speed range. Figure 19 shows that both C_{m_δ} and $C_{m_{C_L}}$ are more positive for the wind-tunnel tests at the lower lift coefficients. These two effects tend to cancel, and thus the agreement with flight is good. At the higher lift coefficients, $C_{m_{C_L}}$ is much more negative for flight, while C_{m_δ} values are about the same, and hence the predicted stability is too great.

The control-force curves of figure 18 show stick-free stability in all cases. The slopes are of the same order above trim speed, but at low speeds the pull forces for flight are much greater with the center of gravity at 0.229 and 0.265 M.A.C. Figure 20 shows a more positive $C_{h_{C_L}}$ for the wind-tunnel tests, and a more negative C_{h_δ} for up-elevator angles. These effects, combined with that due to $\Delta(d\delta_e/dC_L)$, tend to cancel, and give fair agreement of the resultant force curves in most cases. At low speeds with the center of gravity at 0.229 M.A.C. and 0.265 M.A.C., however, the large up-elevator angles and large down-tab angles result in a great loss of tab effectiveness in flight, and hence the flight pull forces are much greater. Some idea of the settings at which the tab effectiveness $C_{h_{\delta_m}}$ begins to decrease rapidly can be gained from figure 21, in which these tab settings are plotted as a function of elevator angle. These data were obtained from the plots of control force and elevator angle against tab setting.

Approach condition (figs. 22, 23, and 24).- Stick-fixed stability is indicated by all the elevator-angle curves of figure 22, and the agreement between wind-tunnel and flight tests is good. Although there are irregularities at large lift coefficients, in general the values of both $C_{m_{C_L}}$ and C_{m_δ} measured in the wind tunnel are more positive than for flight (fig. 23). The tendency of these effects to

balance each other leads to good agreement in the resultant values of $d\delta_e/dC_L$.

The control-force curves of figure 22 show stick-free stability in all cases except at low speeds with the center of gravity at 0.314 M.A.C., and the agreement between predicted and flight data is very good. This agreement is due to the fact that, although there are differences in $C_{h_{C_L}}$, C_{h_δ}, and $d\delta_e/dC_L$ (figs. 24 and 22), the differences are small and the effects tend to cancel.

Differences in longitudinal-stability derivatives.- During the tests and preparation of the data presented, it became apparent that numerous factors would make correlation difficult for this airplane. Undesirable characteristics of the airplane, such as the generally large elevator and rudder control forces, and control friction, made it hard to obtain accurate and consistent data in flight. Physical differences between the airplane and the model, necessary because of the small model scale, included the omission of tabs from the control surfaces and slight differences in the elevator flap. These factors, combined with the possible errors due to control friction, large mass unbalance, and changes in tab effectiveness, made accurate predictions of elevator control forces especially difficult. The flight T_c - C_L relationships for the various power conditions could only be approximated from manifold pressure and engine speed as the airplane was not equipped with thrustmeters or torquemeters, and, due to the large effect of power on the stability characteristics of the airplane, this led to discrepancies between predicted and flight-test results.

For all conditions, the differences in stick-fixed stability as measured by $d\delta_e/dC_L$ are due chiefly to differences in $C_{m_{C_L}}$ at large lift coefficients. For the climb condition (fig. 16), the more negative $C_{m_{C_L}}$ for the wind tunnel is probably due to a local stall over the model wing root. This causes a decrease in downwash over the tail and a resultant increase in stability. It is possible that for the glide, landing, and approach conditions the thrust coefficients used in the predictions are higher than those actually present in flight. These differences, which are due primarily to the errors in calculations of flight thrust coefficients at low manifold pressures and low airspeeds, may result in more positive predicted values of $C_{m_{C_L}}$ at large

lift coefficients as measured in the wind tunnel. The effect
is especially evident for the landing condition (fig. 19),
for which calculations based on model-propeller data and
flight-propeller speed indicated negative flight thrust coef-
ficients (approx. T_c = -0.04). The differences in stick-
free stability, as indicated by the variation of control
force with airspeed, do not appear to be controlled by any
one factor. The summation of the effects of $\Delta(d\delta_e/dC_L)$,
ΔC_{hC_L}, and $\Delta C_{h\delta}$ depends on the condition, airspeed range,
and center-of-gravity location, and in general the effects
tend to cancel. The only situation in which $\Delta d\delta_e/dC_L$ has
a large effect is at low speeds in the climb condition, where,
as explained previously, the more stable $d\delta_e/dC_L$ for the
predictions is due to more negative C_{mC_L} values. The
differences in C_{hC_L} as measured in the wind tunnel and as
estimated from flight are not consistent for all conditions,
and are probably within the accuracies which can be obtained
with the test and calculation methods which were used. The
previously mentioned inability to match perfectly the power
conditions no doubt leads to some error in C_{hC_L} as, for
example, in the landing condition (fig. 20). The values of
$C_{h\delta}$ measured in the wind tunnel were greater in all cases
than those estimated from the flight data, although for down-
elevator angles the discrepancies are small. Little change
in either $C_{m\delta}$ or $C_{h\delta}$ is shown between up- and down-elevator
angles for the flight tests, while the wind-tunnel tests show
much more negative values of $C_{m\delta}$ and $C_{h\delta}$ in all cases.
The major portion of this change is believed to be due to the
difference between the model and the airplane elevator flaps.
Air flow through the model elevator-flap gap probably caused
some of the increase in the elevator effectiveness and changed
the pressure distribution so that the hinge moments were
increased.

Elevator Control in Turning Flight

The elevator-angle gradients in figure 25 show good
agreement between flight and predictions. The control-force
gradients, which in all cases are excessive, are in fair
agreement except for the forward (0.240 M.A.C.) center-of-
gravity location.

It is not possible, due to the greater number of
variables involved, to analyze this turning-flight data from

a coefficient standpoint in the detailed manner used for the
static-longitudinal-stability discussion. Satisfactory
correlation in elevator-angle gradients would be expected,
as the $C_m - C_L$ relationships indicate good agreement in the
glide condition (fig. 13) and in the climb condition at the
lower lift coefficients (fig. 16). It appears that the allow-
ances made for the curvature of the flight path, changes in
the $T_c - C_L$ relationships, and $C_{m_{1m}}$ were sufficiently
accurate to permit satisfactory predictions. The many factors
and stability derivatives which affect the control-force
gradients are such that fair agreement results from the pre-
dictions. Most of the increase over the flight values of the
predicted control-force gradient with center of gravity at
0.240 M.A.C. may be attributed to the large negative C_{h_δ} for
the wind-tunnel tests with up-elevator angles.

Elevator Control in Landing

Although the agreement in absolute values of elevator
angle is erratic, the data presented in figure 26 for both the
flight and wind-tunnel tests indicate that sufficient elevator
control is available for low-speed landings over the center-of-
gravity range, but that the corresponding elevator control
forces are excessive.

Most of the flight-test landing approaches were made with
power on and the throttles were cut back prior to ground
contact. Examination of the instrument records showed that in
the test landings with the center of gravity at 0.316 M.A.C.
(fig. 26(b)) the engines were throttled comparatively early in
the approach so that the power conditions at contact were very
similar to those used in the landing-condition stability test
at altitude. In many of the landings with the center of gravity
at 0.224 M.A.C. (fig. 26(a)), however, the engines were throttled
only several seconds before contact, and the power conditions
at contact were thus somewhat variable.

The predicted values of elevator angle presented in
figure 26 are greater than for flight. Both methods (model
tested in the presence of a ground board and computed ground
effect) used in the predictions gave similar values. The
flight curves show little change for the forward center-of-
gravity location between the values obtained at 6,000 feet
(fig. 18(a)) and those obtained during landing (fig. 26(a)).

The reasons for the small ground effects in flight are not apparent. The dynamic factors in the flight tests were small and inconsistent. It is not believed that they would account for the smaller ground effect experienced in flight as compared with that obtained in the wind tunnel. Difficulty was encountered in making the landings due to high control forces, and consequently the landing technique varied somewhat from flight to flight. Stalling of the tab at the large down-tab and up-elevator angles may result in some reduction in the up-elevator angle required.

The correlation between predicted and flight values of elevator control force for landings (fig. 26) is very good with respect both to the slopes of the curves and to the absolute values of force. For the purpose of comparison, the tab setting used in the predictions was that which gave zero control force at the same contact speed as for the flight tests. As was the general case for the control forces in the stability tests, the differences in the various factors (including ground effect) which influence the control forces tended to balance each other and this resulted in satisfactory correlation. The larger pull forces indicated in figure 18 for the stability flight tests at altitude with the forward center-of-gravity location apparently were compensated by the greater predicted up-elevator angles required in landing.

CONCLUSIONS

Based on the data presented in this report, the following conclusions can be drawn with regard to the correlation of the longitudinal-stability and -control characteristics of a twin-engine patrol airplane as measured in flight and as predicted from wind-tunnel tests.

1. The wind-tunnel predictions indicated critical unsatisfactory longitudinal-stability and -control characteristics, the most serious of which were the large elevator control forces in maneuvering flight and in landings.

2. The chief reasons for the unsatisfactory characteristics and possible methods of improvement can be deduced from the wind-tunnel data.

3. Careful simulation of the actual airplane, with regard both to the model (especially the control surfaces) and to the control-system characteristics (mass unbalance, boost-tab ratio, mechanical advantage, etc.) used in the computations, is necessary for satisfactory predictions.

4. Accurate information on the flight conditions and operating techniques must be available for the predictions. The power conditions were especially critical on this airplane, due to the large effects of power on longitudinal stability.

5. The aerodynamic longitudinal-stability derivatives as estimated from flight-test data and as measured in the wind tunnel were, in general, in good agreement. The differences were partially due to physical dissimilarities between the model and airplane and to imperfect matching of power conditions.

Ames Aeronautical Laboratory,
    National Advisory Committee for Aeronautics,
        Moffett Field, Calif.

REFERENCES

1. Stevens, Victor I., Jr., and McCullough, George B.:
   Flying Qualities of the PV-1 as Estimated from Wind-
   Tunnel Tests. NACA CMR, Sept. 1943.

2. Anon.: Erection and Maintenance Instructions for Army
   Model RB-34 Series, British Models Ventura BI, II,
   IIA, and IV Airplanes. Technical Order No. 01-55EA-2,
   Nov. 1943 (revised April 1944).

3. Goett, Harry J., Jackson, Roy P., and Belsley, Steven E.:
   Wind-Tunnel Procedure for Determination of Critical
   Stability and Control Characteristics of Airplanes.
   NACA ARR No. 4D29, 1944.

4. Ames, Milton B., Jr., and Sears, Richard I.: Deter-
   mination of Control-Surface Characteristics from
   NACA Plain-Flap and Tab Data. NACA Rep. No. 721.
   1941.

5. Katzoff, S., and Sweberg, Harold H.: Ground Effect on
   Downwash Angles and Wake Location. NACA Rep. No. 738,
   1943.

TABLE I.- GENERAL CHARACTERISTICS OF THE AIRPLANE

Normal gross weight . . . . 26,500 lb	
Center-of-gravity locations	
Normal (gear up) . . . . 0.298 M.A.C.	
Normal (gear down). . . . . 0.287 M.A.C.	
Most forward allowable (gear down). . . . . 0.235 M.A.C.	
Most rearward allowable (gear up) . . . . . 0.331 M.A.C.	
Maximum allowable maneuvering load factor	
(for normal gross weight) 3.1	
Control-wheel diameter. . . . . 14 in.	
Engines 2	
Make. . . . . Pratt and Whitney R-2800-31	
Propeller-gear ratio. 16:9	
Propellers	
Make. . . . . Hamilton Standard, constant speed, blade no. 6477A-12	
Diameter. . . . . .10.50 ft	
Number of blades. . . . . three	
Low-pitch blade stop. . . . . 26°	
High-pitch blade stop . . . . 88°	

TABLE II.— WING AND HORIZONTAL-TAIL-PLANE
DIMENSIONS OF THE AIRPLANE

Item	Wing	Horizontal tail
Area (sq ft)	[1]576	133.96
Span	65.5	25.86
Aspect ratio	7.79	5.00
Taper ratio	[2]3.42:1	-----------
Dihedral	[3]4° $3'$	0°
Incidence (with respect to fuselage reference line)	2°	0°
Root section	NACA 23018	NACA 0013
Tip section	NACA 23009	NACA 0009
Twist (geometric)	None	None
M.A.C. (ft)	[1]10.27	-----------
Root chord	[2]13.78	-----------

[1] Includes trailing-edge extension.
[2] Exclusive of trailing-edge extension.
[3] Measured on top of main beam.

TABLE III.– ELEVATOR AND FLAP SURFACE
DIMENSIONS OF THE AIRPLANE

Item	Elevator		Flaps (Fowler)
	[1]Up	Down	
Area aft of hinge line (sq ft)	40.1	35.1	52.3
Average chord aft of hinge line (ft)	1.97	1.97	3.33
Span (ft)	At hinge line 20.21	At hinge line 17.90	15.72
Balance, type	Boost tab	Boost tab	————
Balance area (sq ft)	5.3	5.3	————
Percent balance	13	15	————
Control travel (deg)	32° up 28° down	32° up 28° down	38° down
Trim-tab area (sq ft)	2.015	2.015	————
Tab span (ft)	4.25	4.25	————
Boost ratio $\Delta\delta_T/\Delta\delta$	−0.36 approx.	−0.36 approx.	————

[1]A tail flap between sections of elevator operates for up-elevator only.
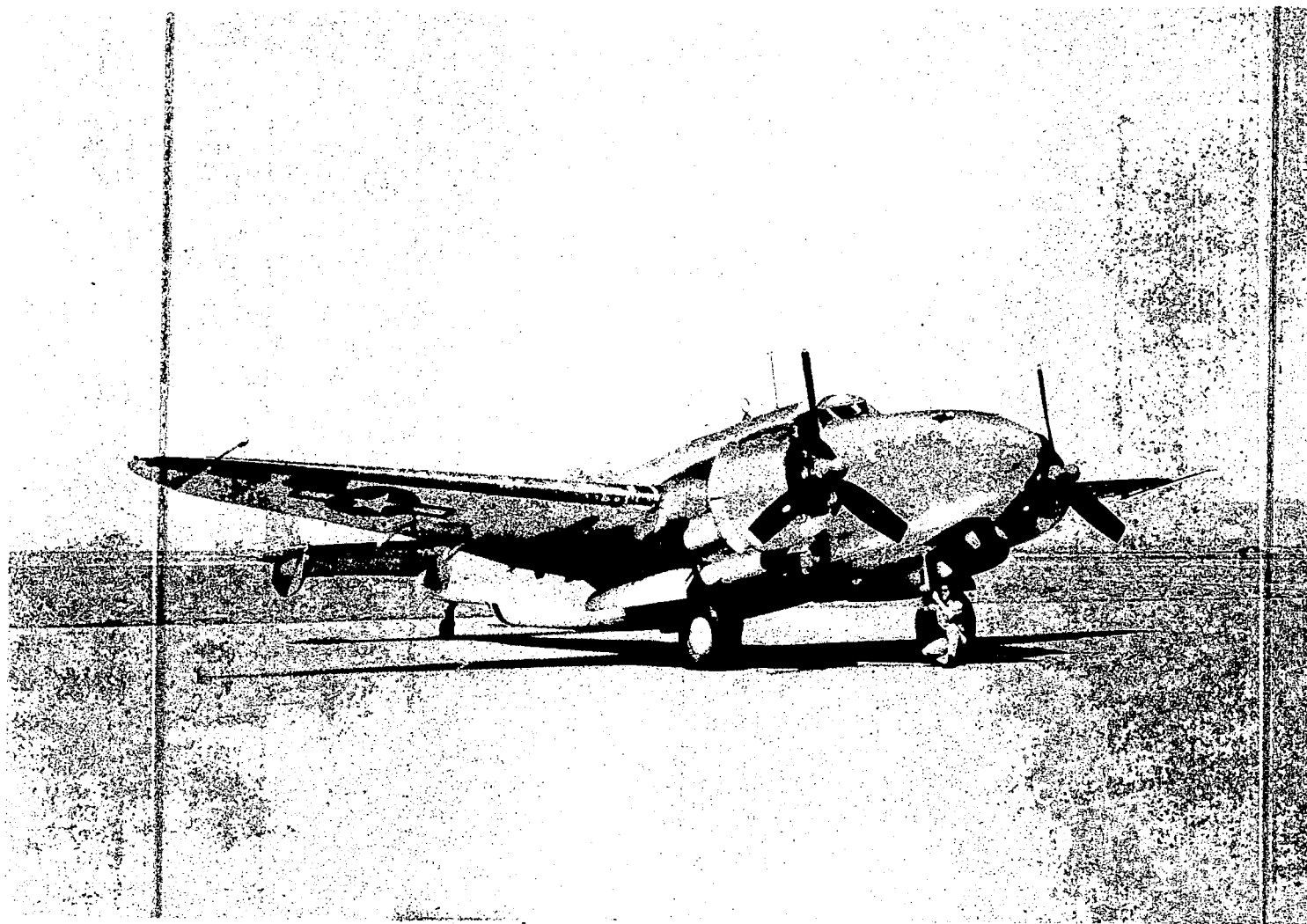
(a) Front view, flaps retracted.

Figure 1. - The airplane as instrumented for flight tests.
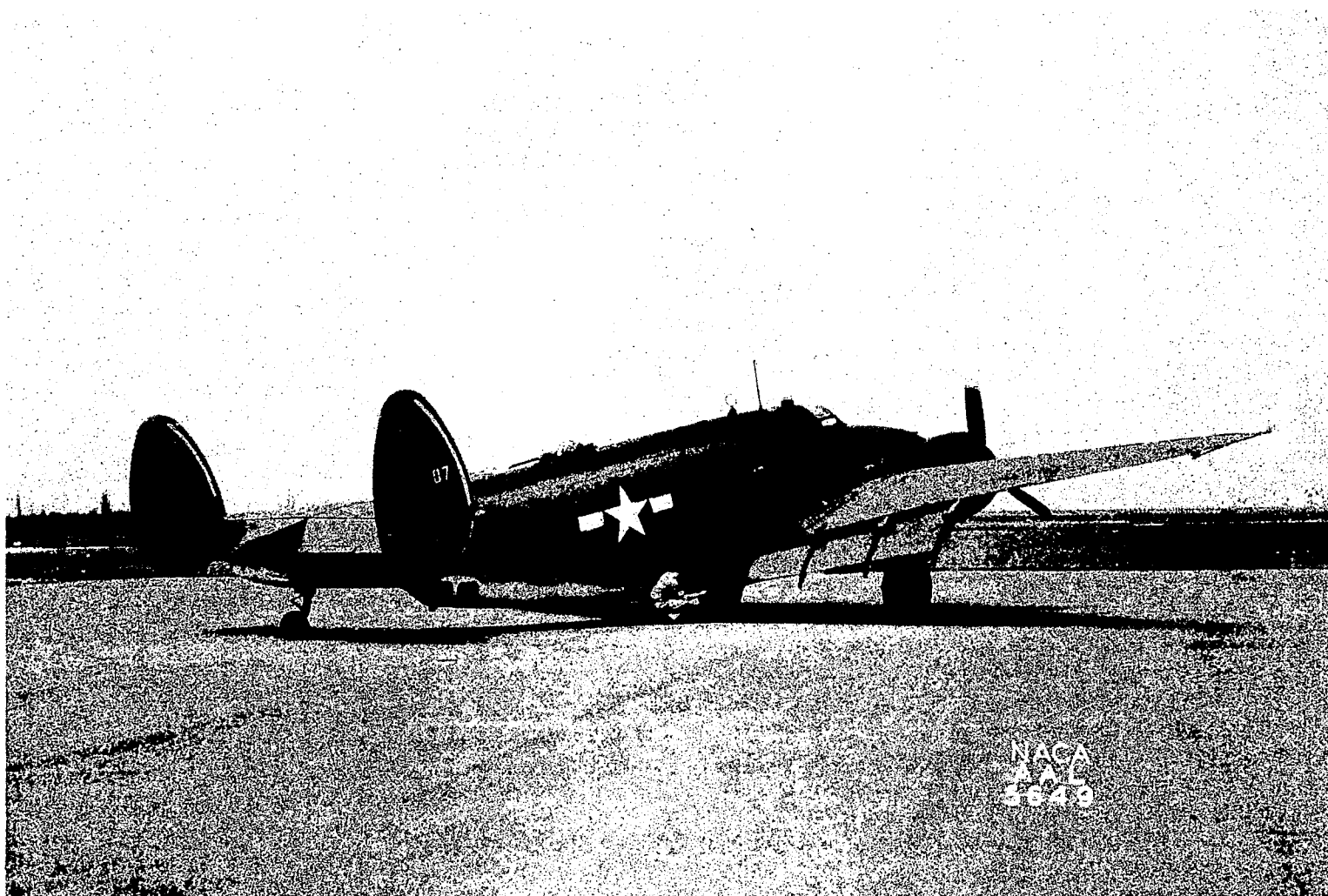
(b) Rear view, flaps deflected.

Figure 1. - Concluded. The airplane as instrumented for flight tests.

51'-0"

65'6"

0   5'   10'
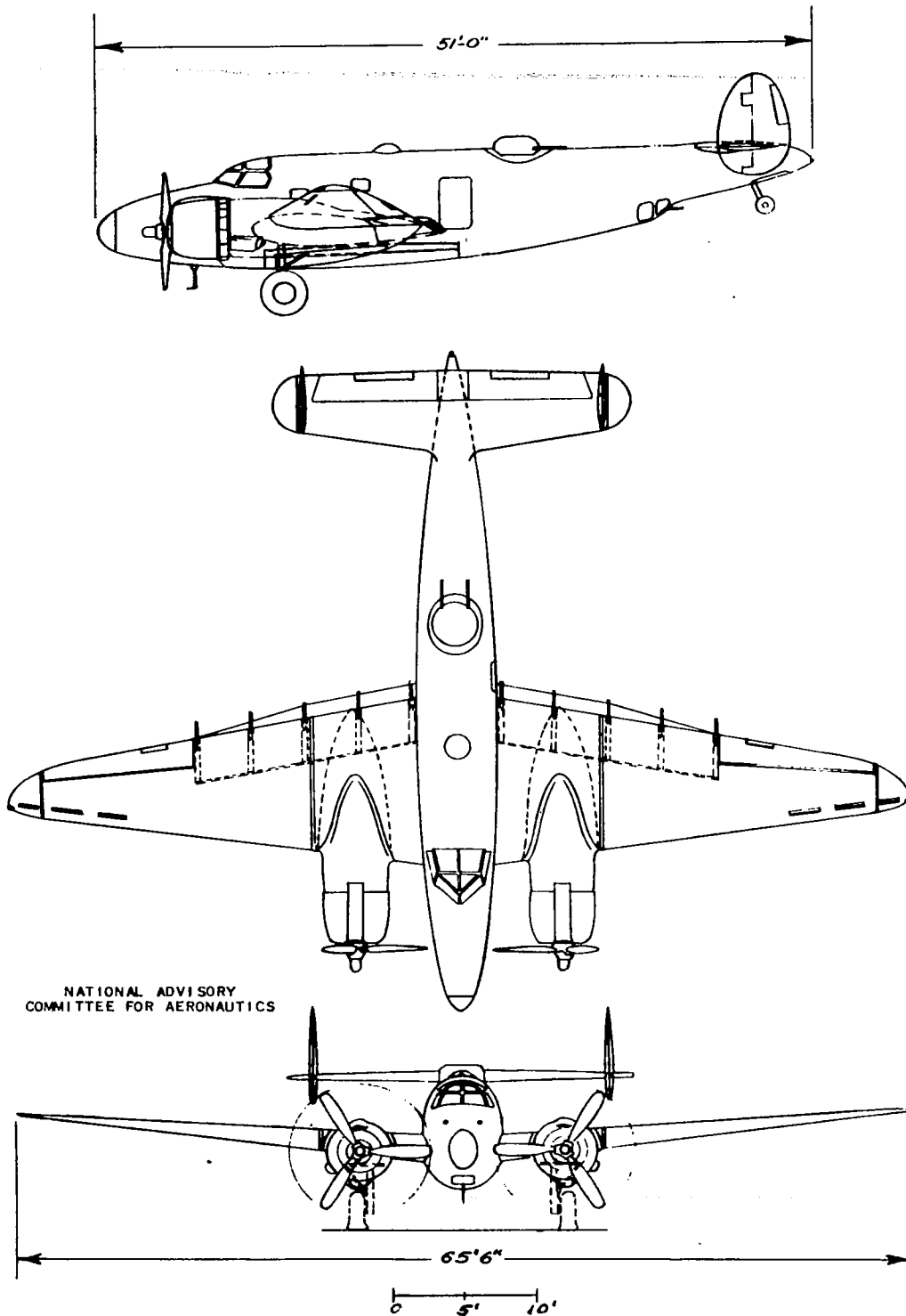
Figure 2. - Three-view drawing of the twin-engine patrol airplane.
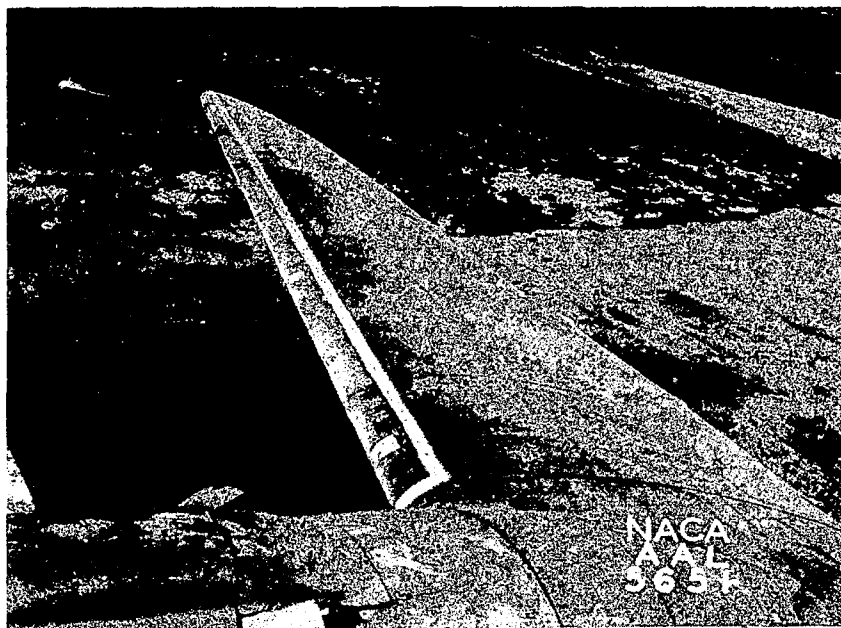
(a) View looking outboard.
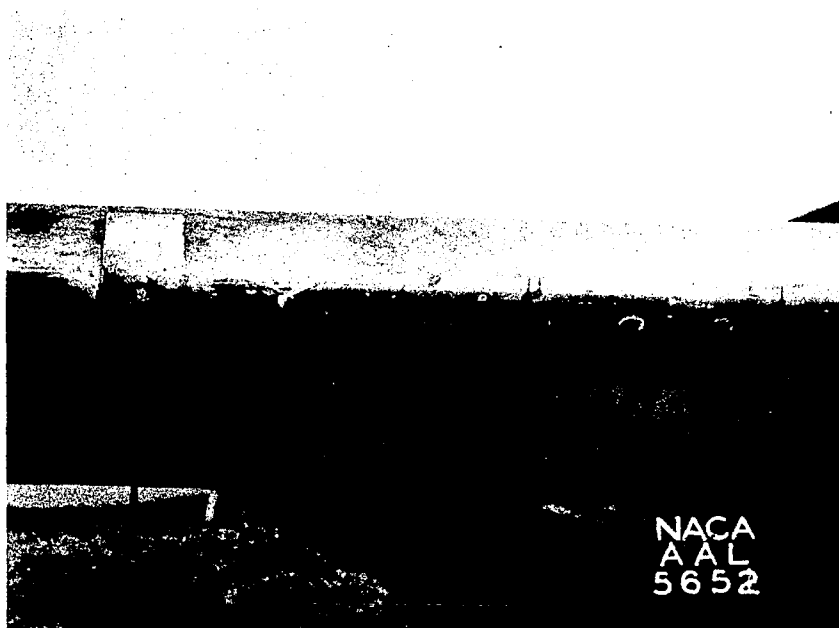
(b) Front view.

Figure 3.- Outer wing panel with de-icer boots removed.
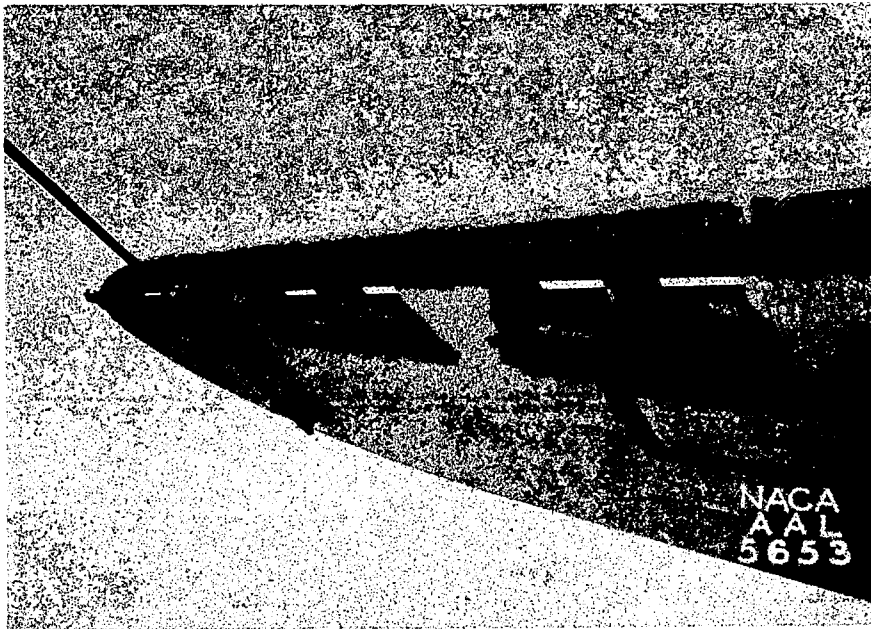
Figure 4.- Details of wing tip with de-icer boots removed.
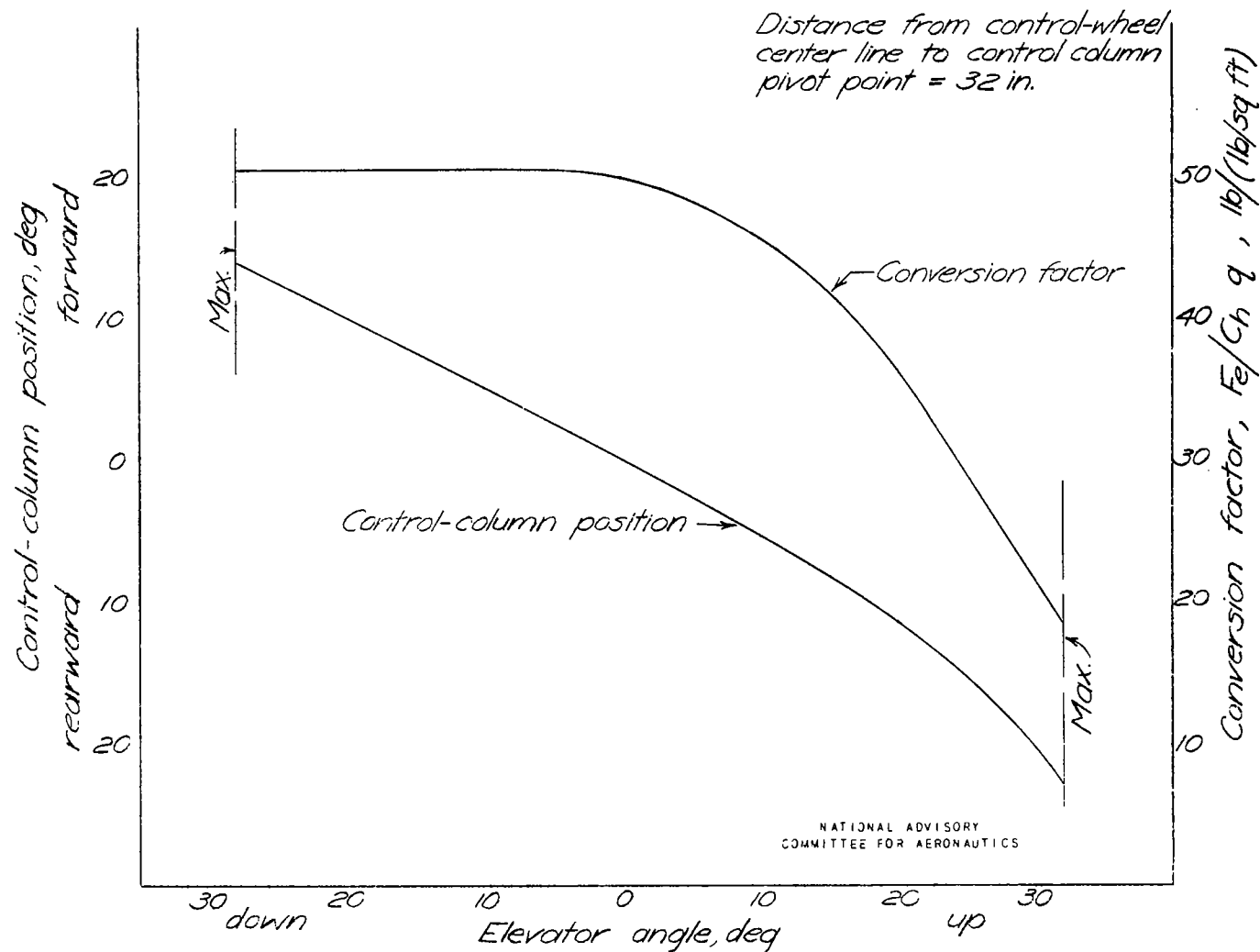
Figure 5 .- Kinematics of the elevator control system as measured on the ground with no load on the surface.
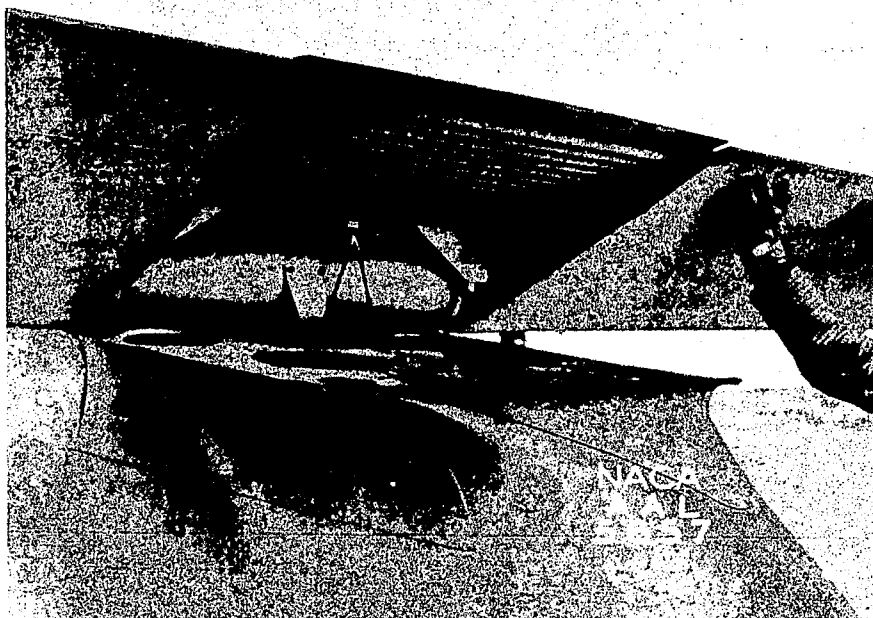
Figure 6.- Details of tail flap.
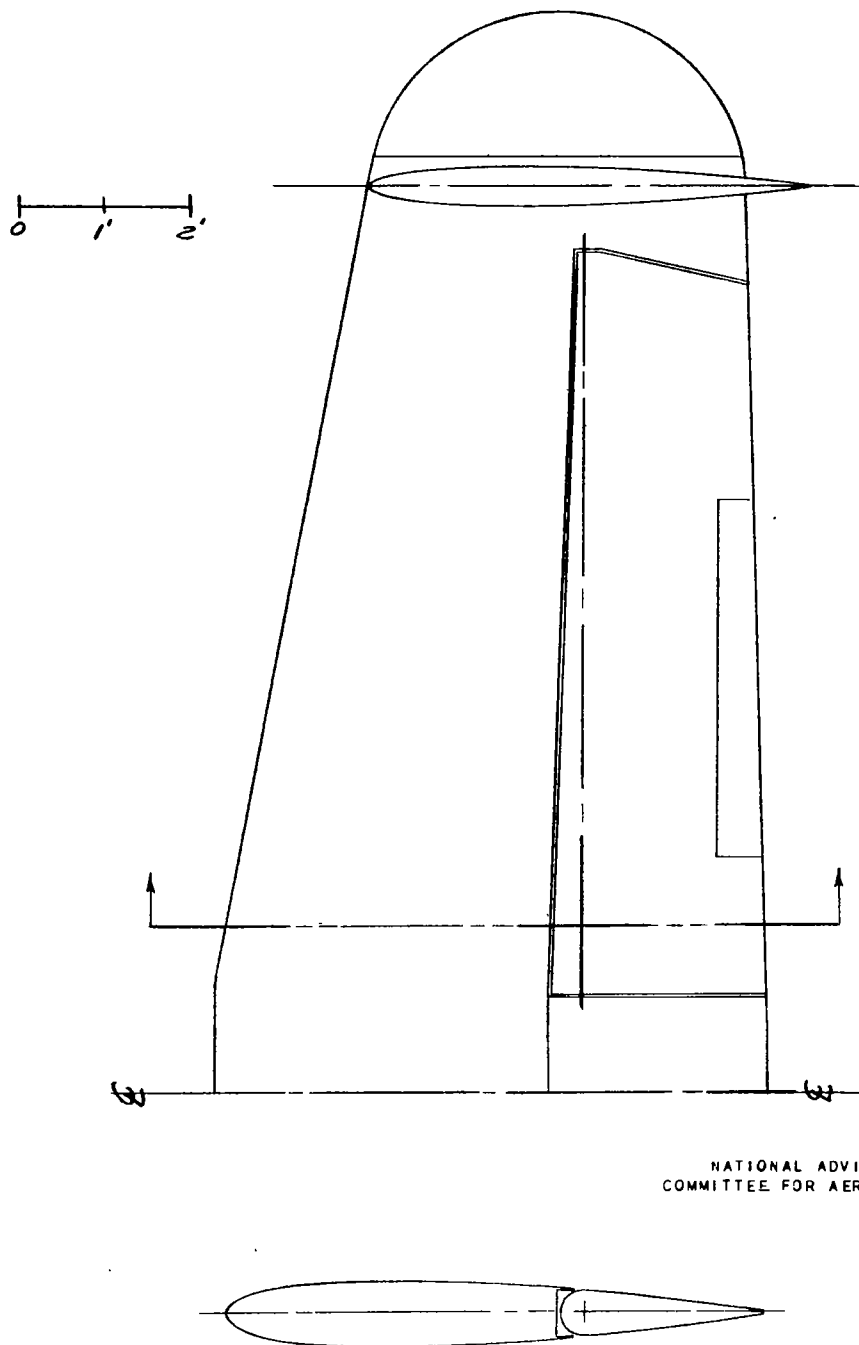
Figure 7.- Sketch of horizontal tail surface of the airplane.
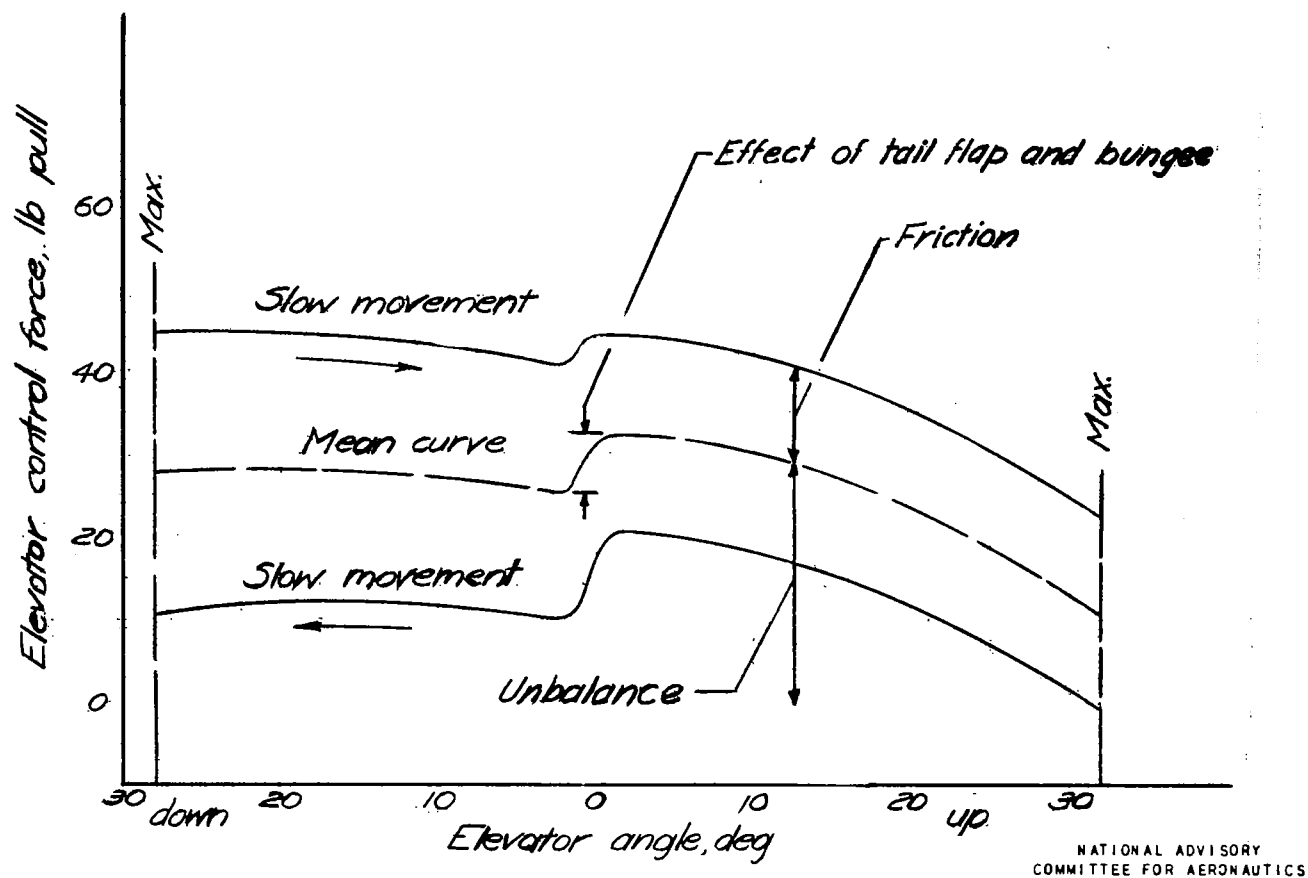
Figure 8 .- Variation of elevator control force with elevator angle, as measured on the ground with no load on the control surfaces.
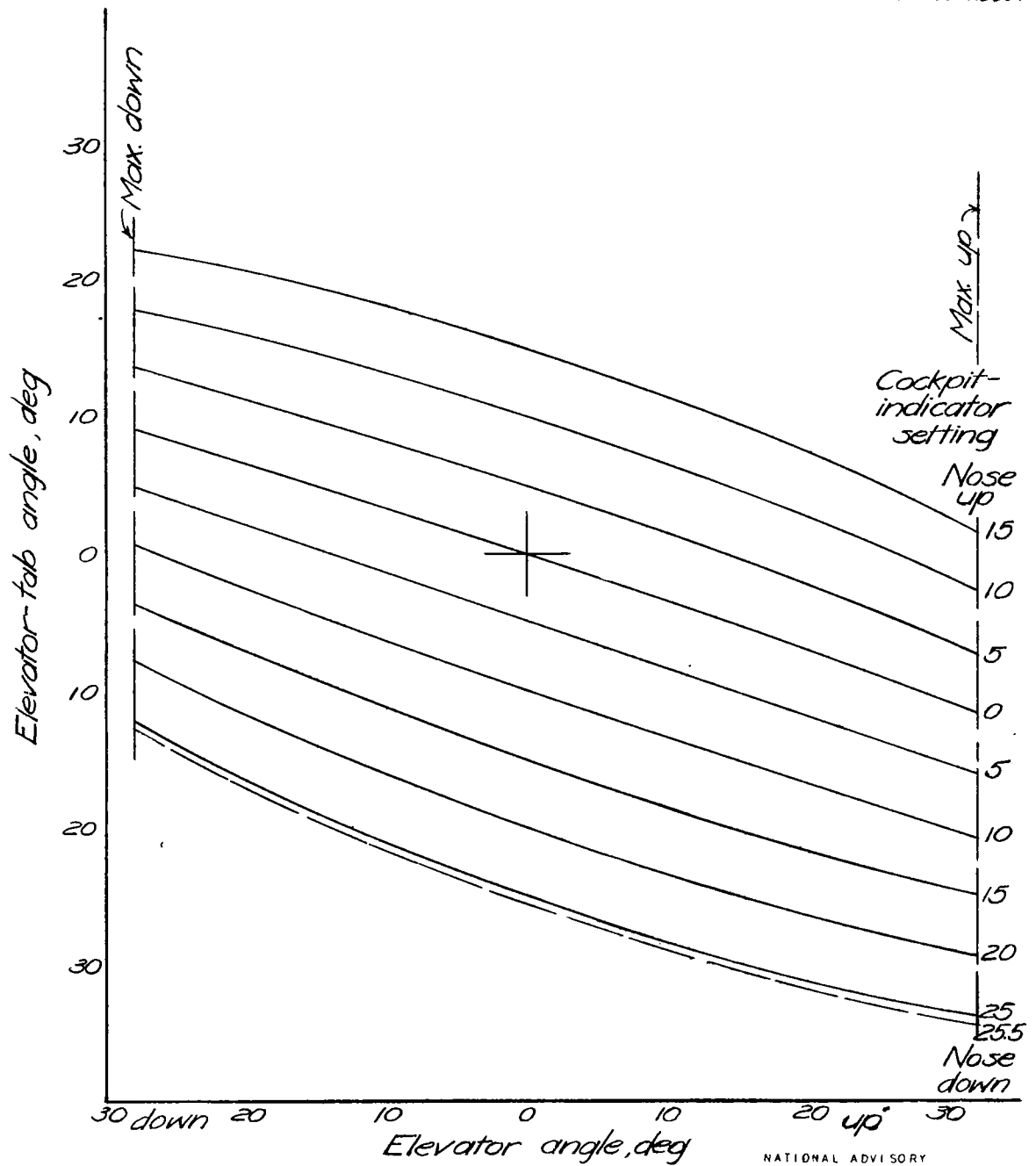
Figure 9 .- Variation of elevator-tab angle with elevator angle at various cockpit-indicator settings.
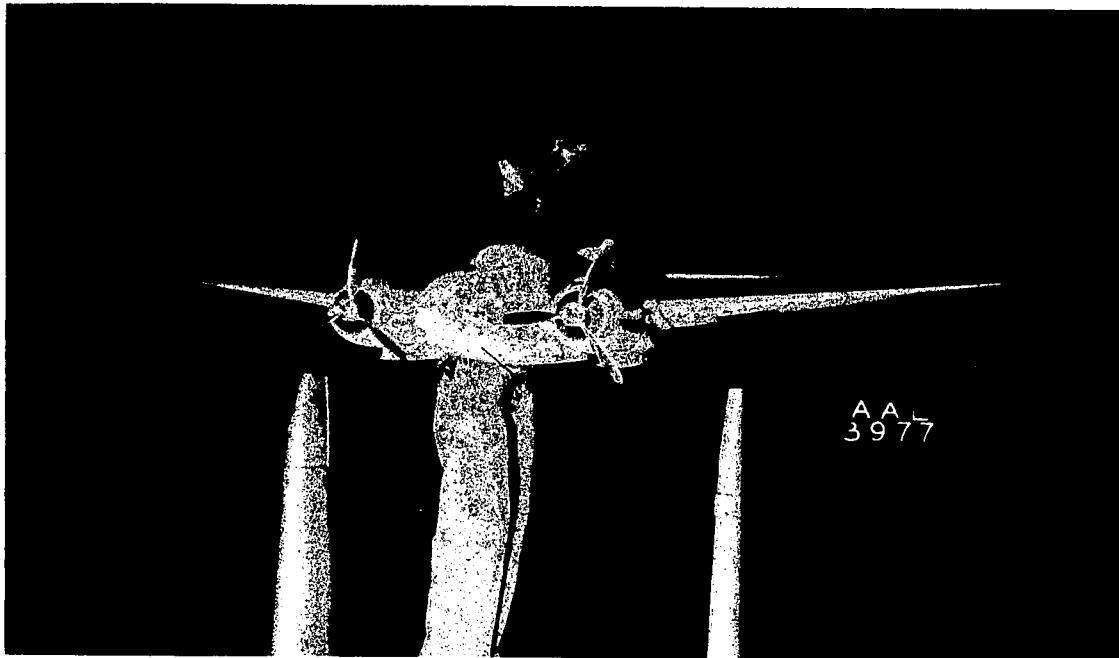
(a) Front view, flaps retracted.
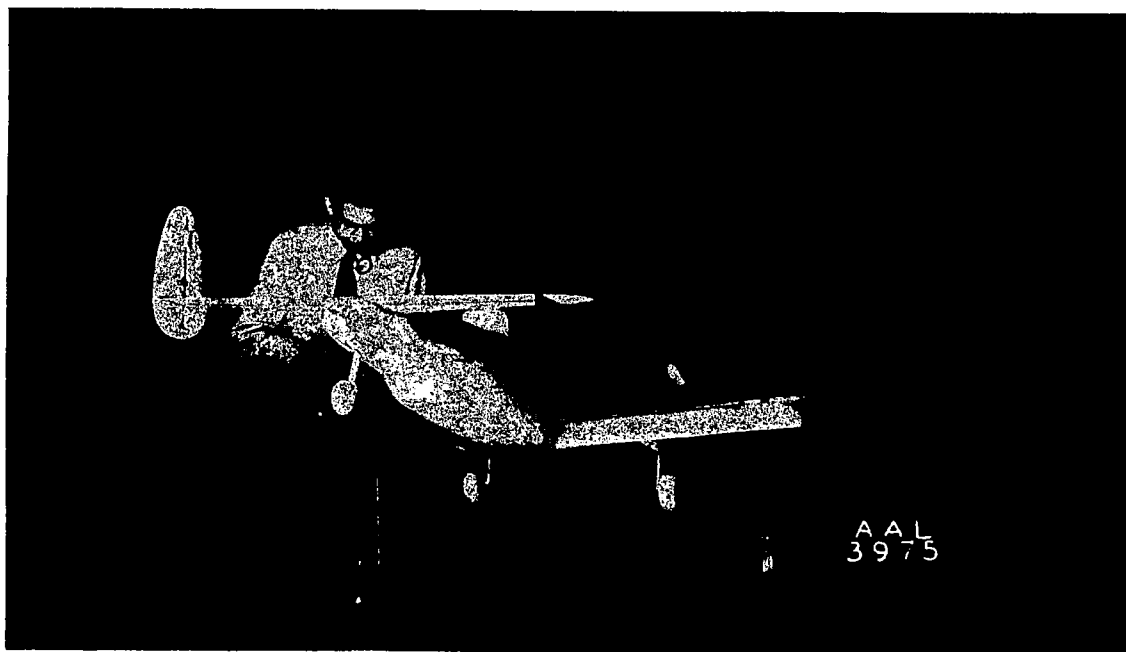
(b) Rear view, flaps down.

Figure 10.- The 1/9-scale model of the airplane mounted in the
7- by 10-foot wind tunnel.
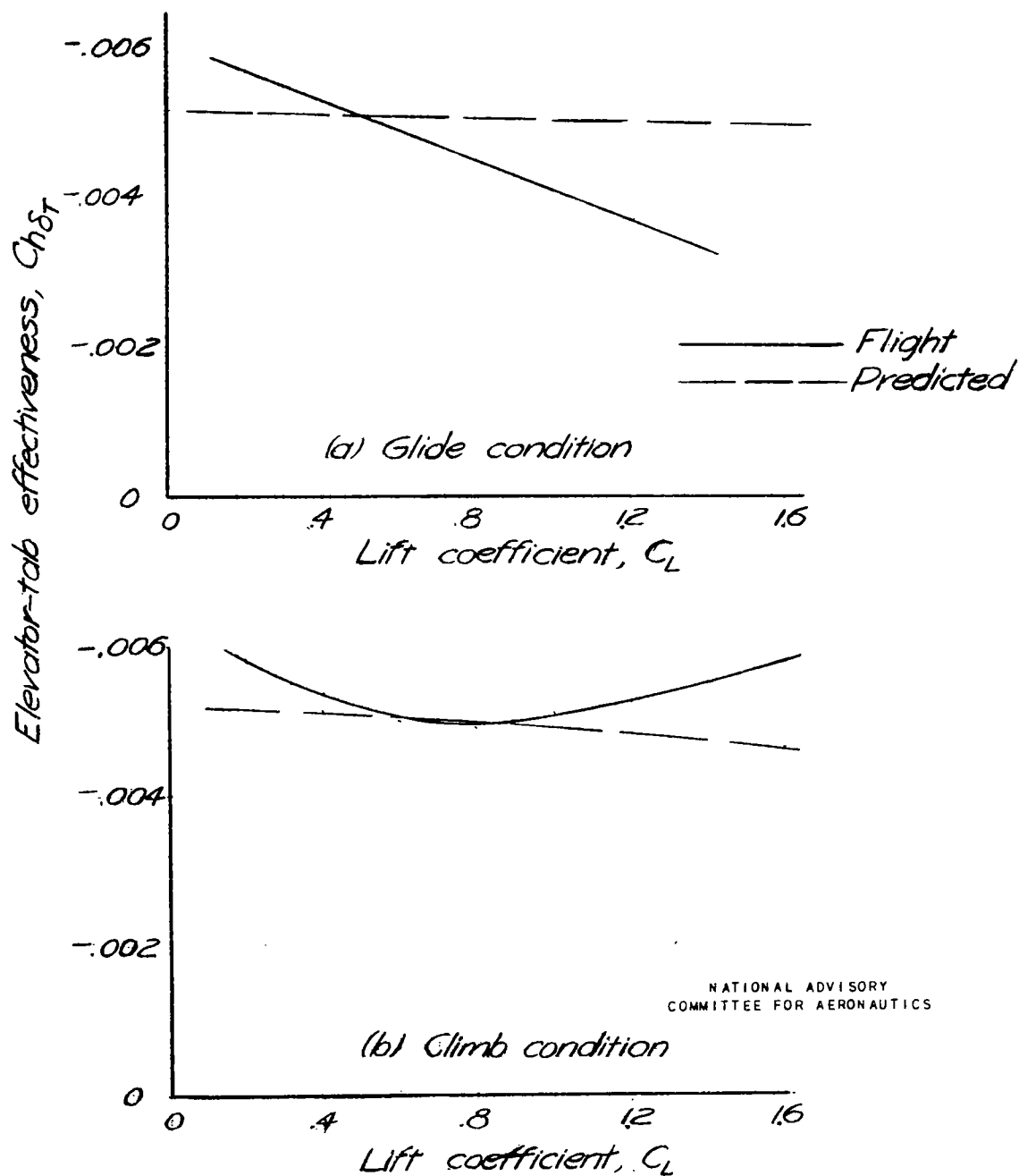
Figure 11.- Variation of elevator tab
effectiveness, $C_{h_{\delta_T}}$, with lift coefficient, C_L.
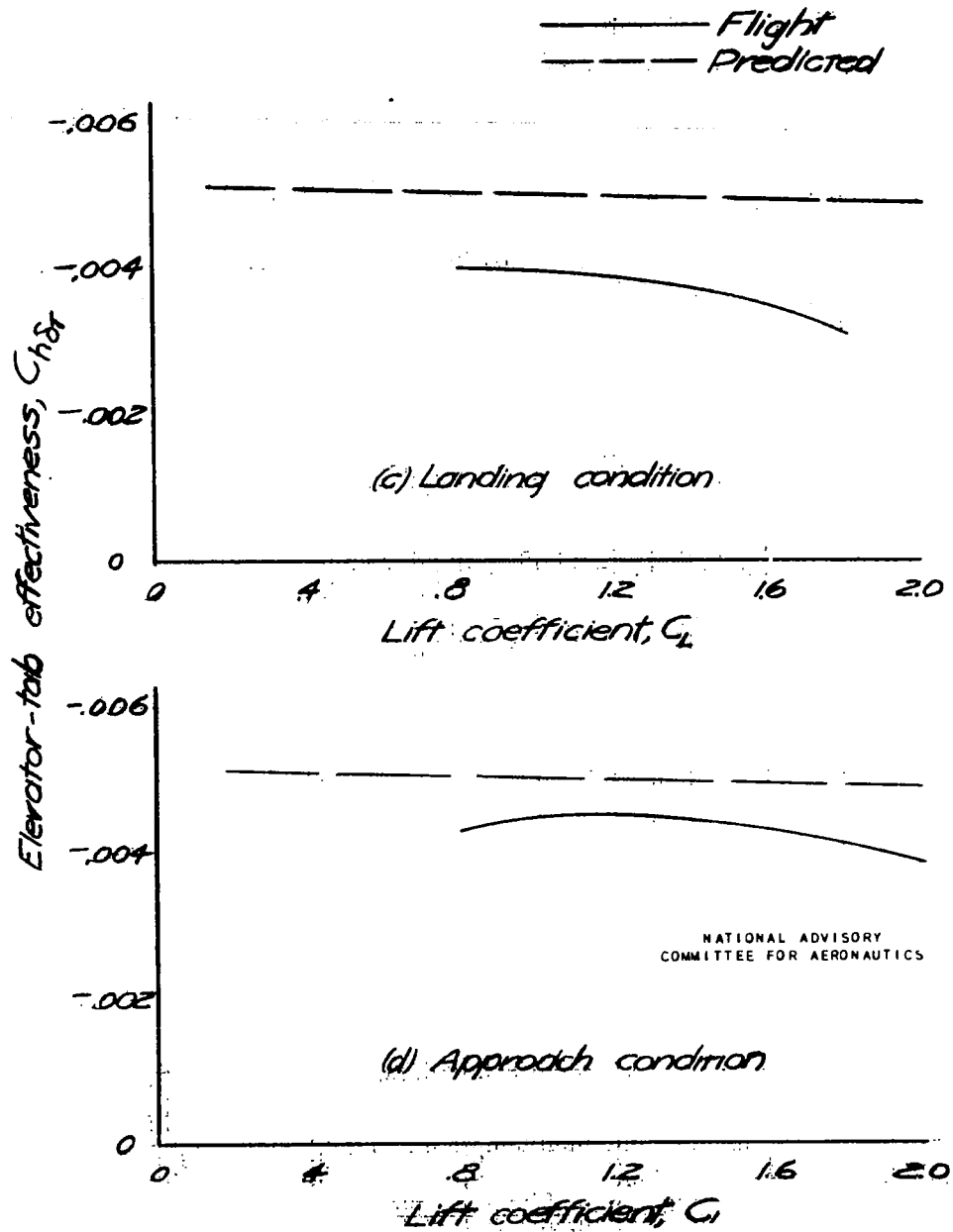
Figure 11 :- Concluded.

(a) c.g. location 0.240 M.A.C.
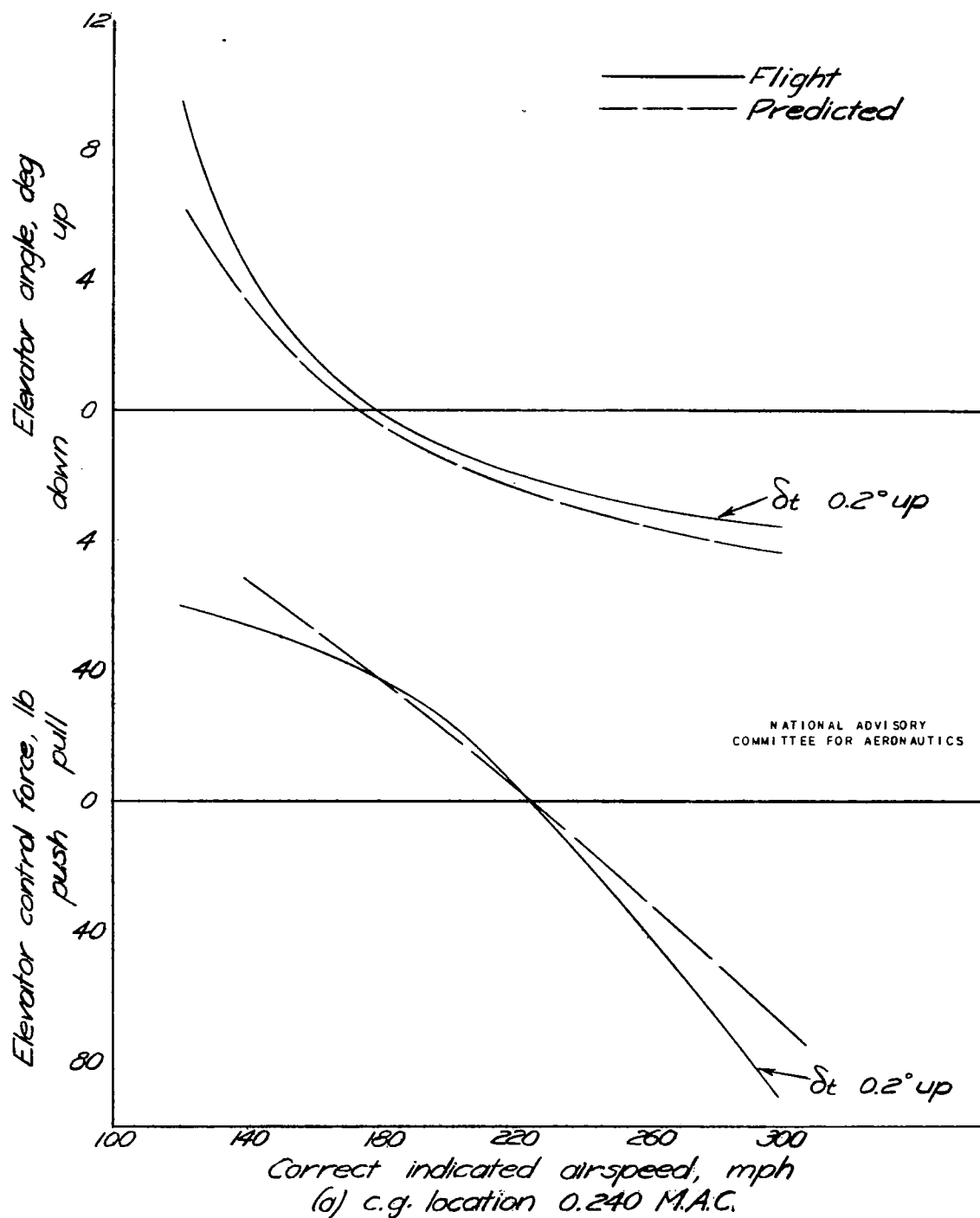
Figure 12 .- Variation of elevator angle and control force with airspeed, glide condition. Steady straight unyawed flight.

Figure 12 .- Glide condition, continued.
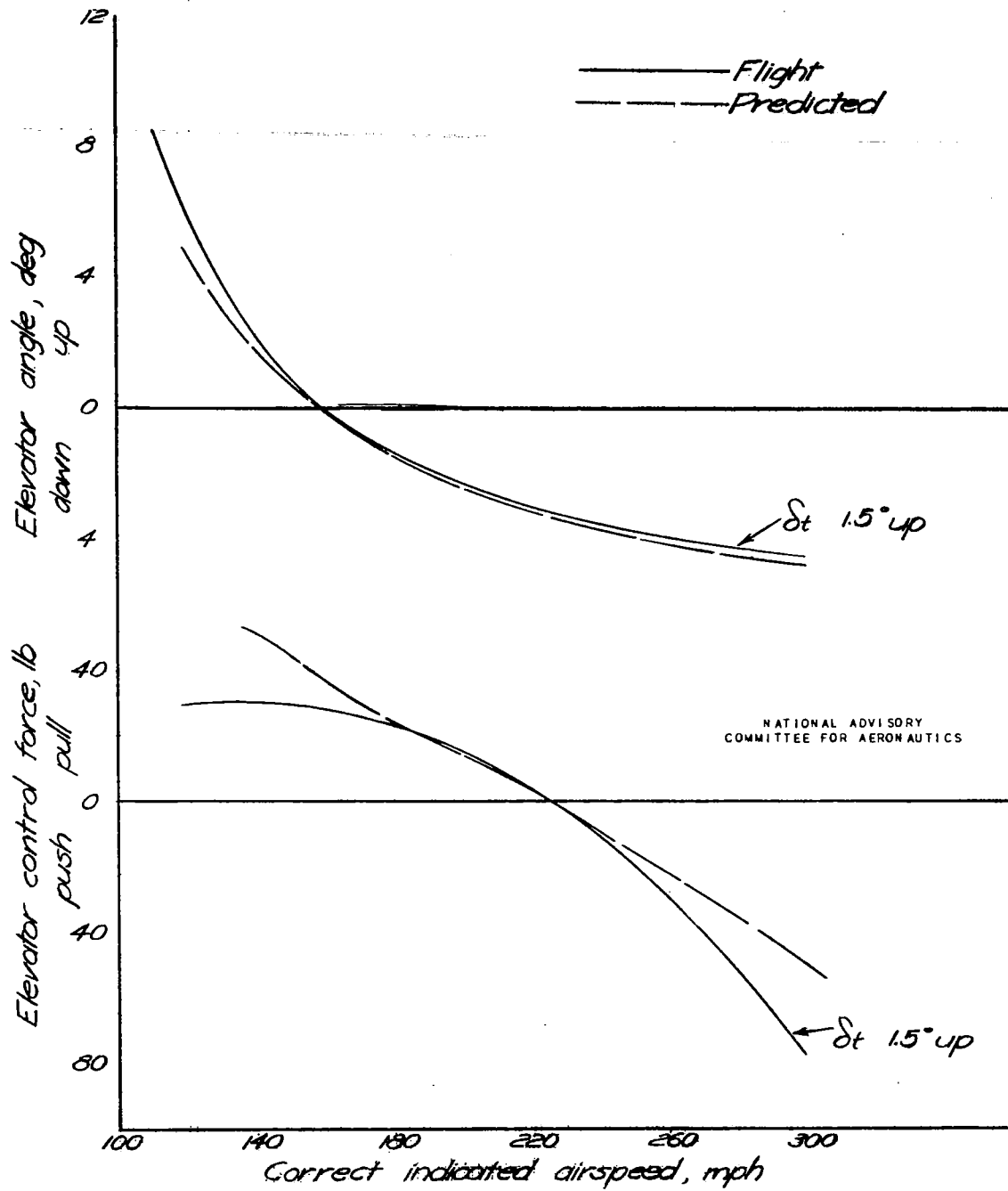
(b) c.g. location 0.274 M.A.C.
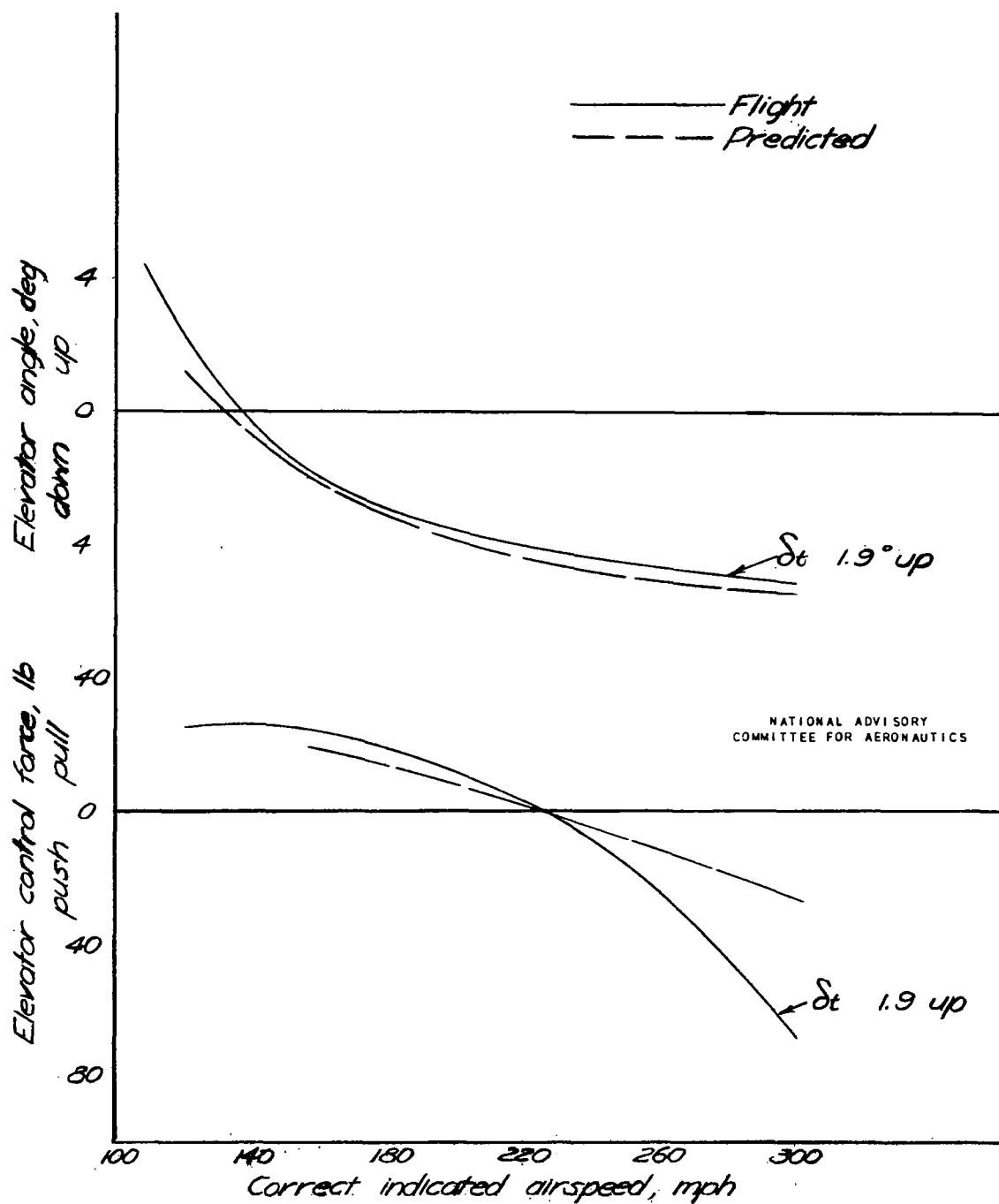
(c) c.g. location 0.323 M.A.C.

Figure 12 – Glide condition, concluded.
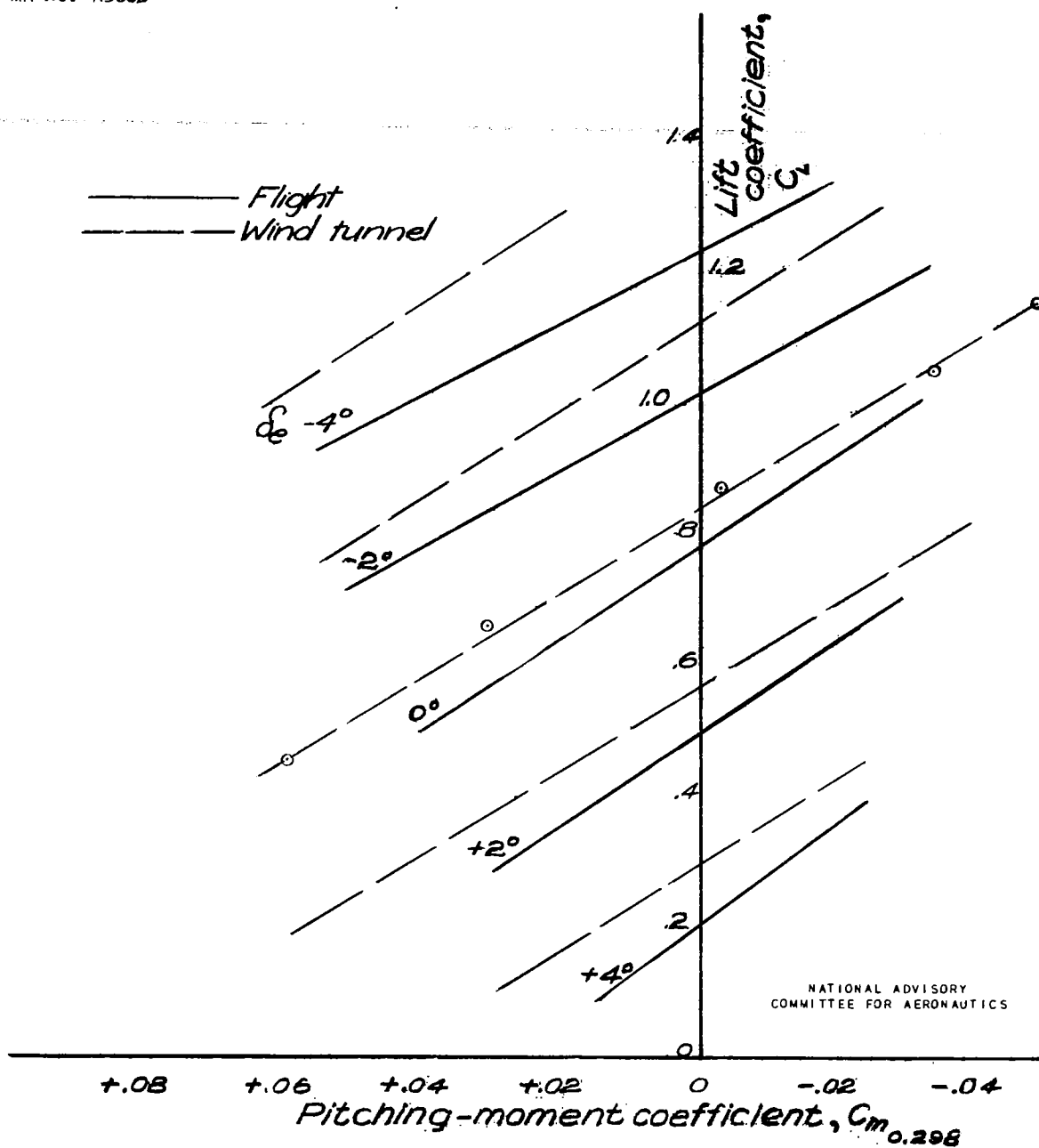
Figure 13 .- Pitching-moment characteristics. Glide condition.
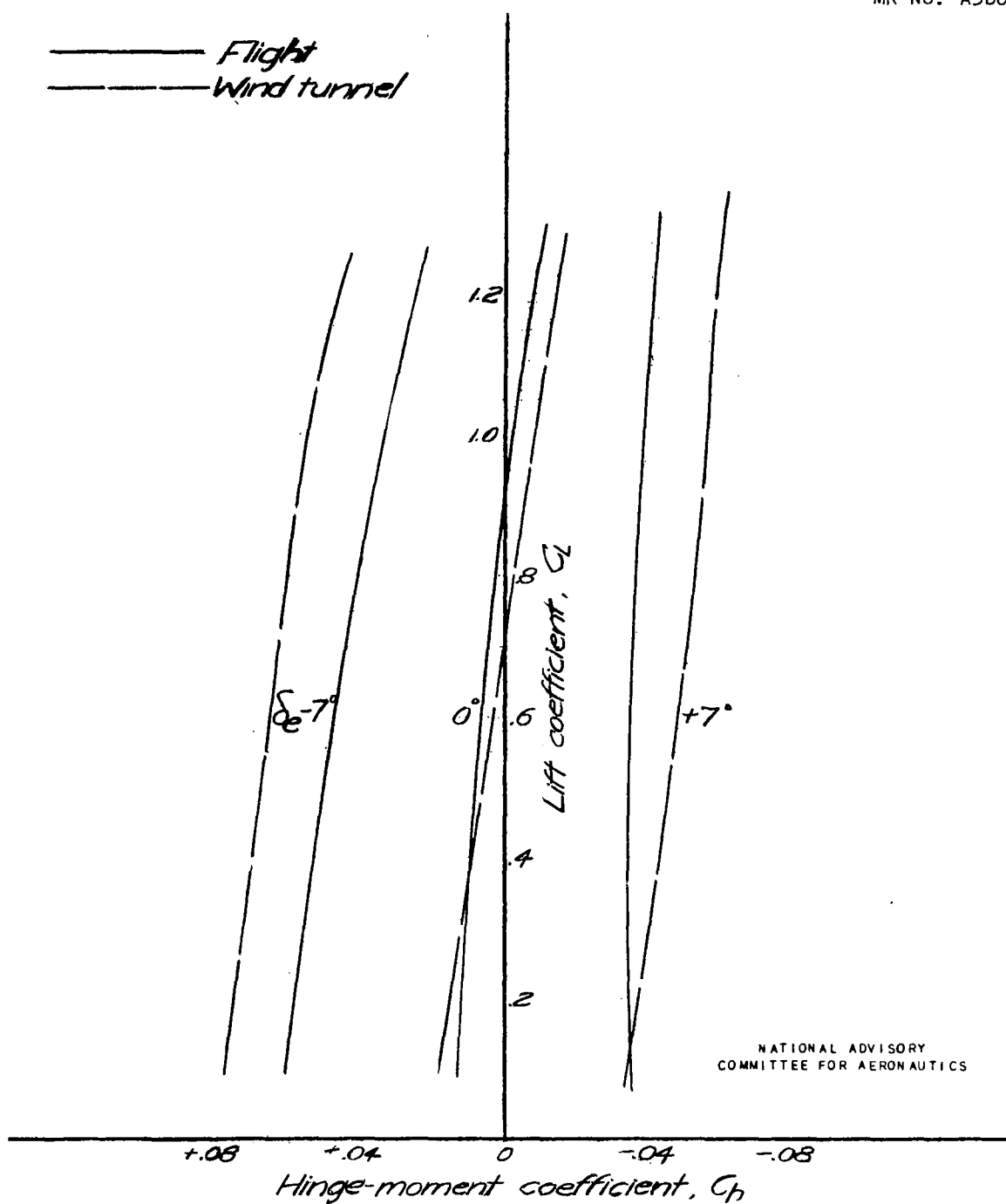
Figure 14 .— Elevator hinge-moment characteristics.
Glide condition.

δt 0.9° up

Flight
Predicted

δt 2.0° down

δt 0.9° up

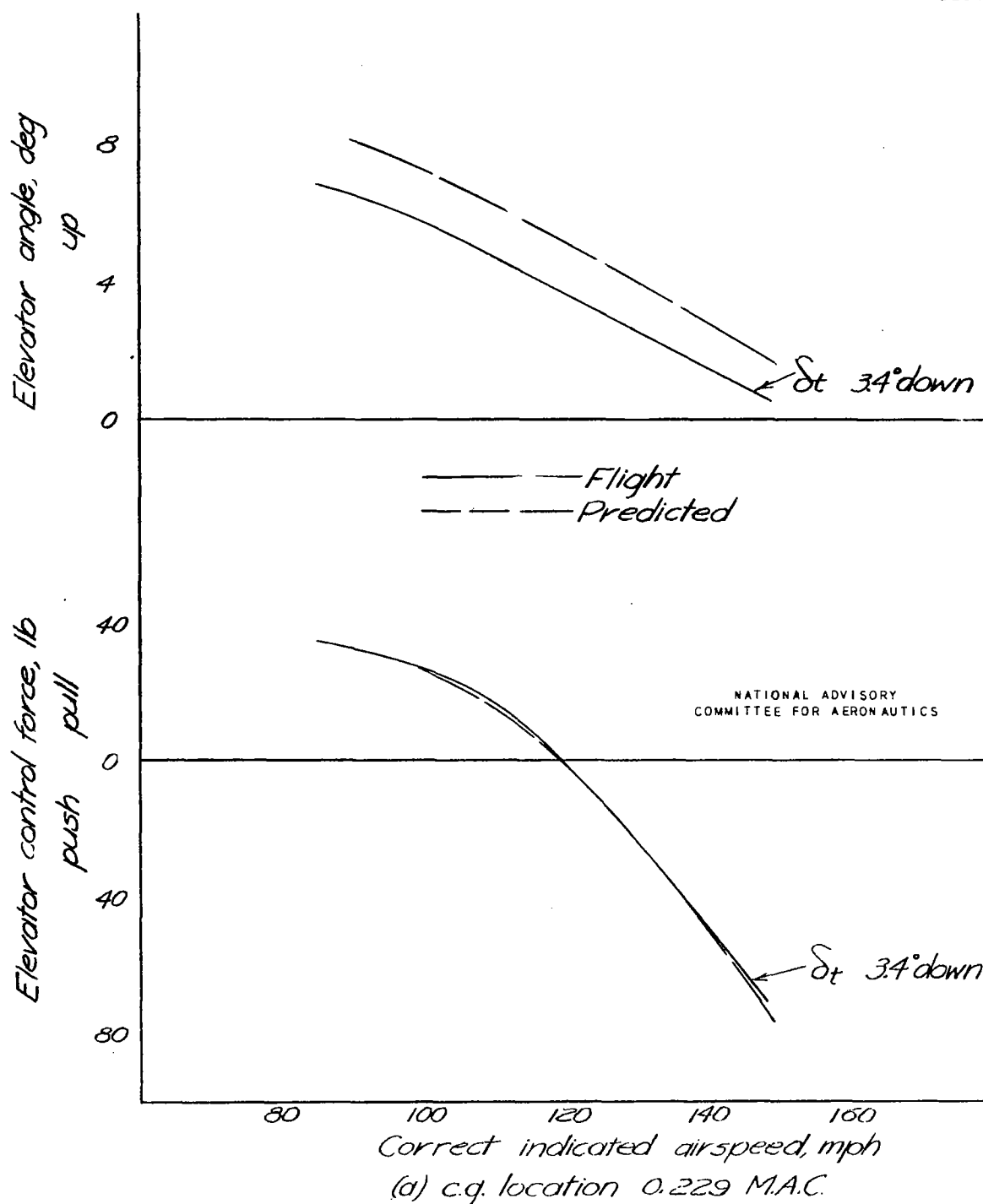Correct indicated airspeed, mph

(a) c.g. location 0.245 M.A.C.
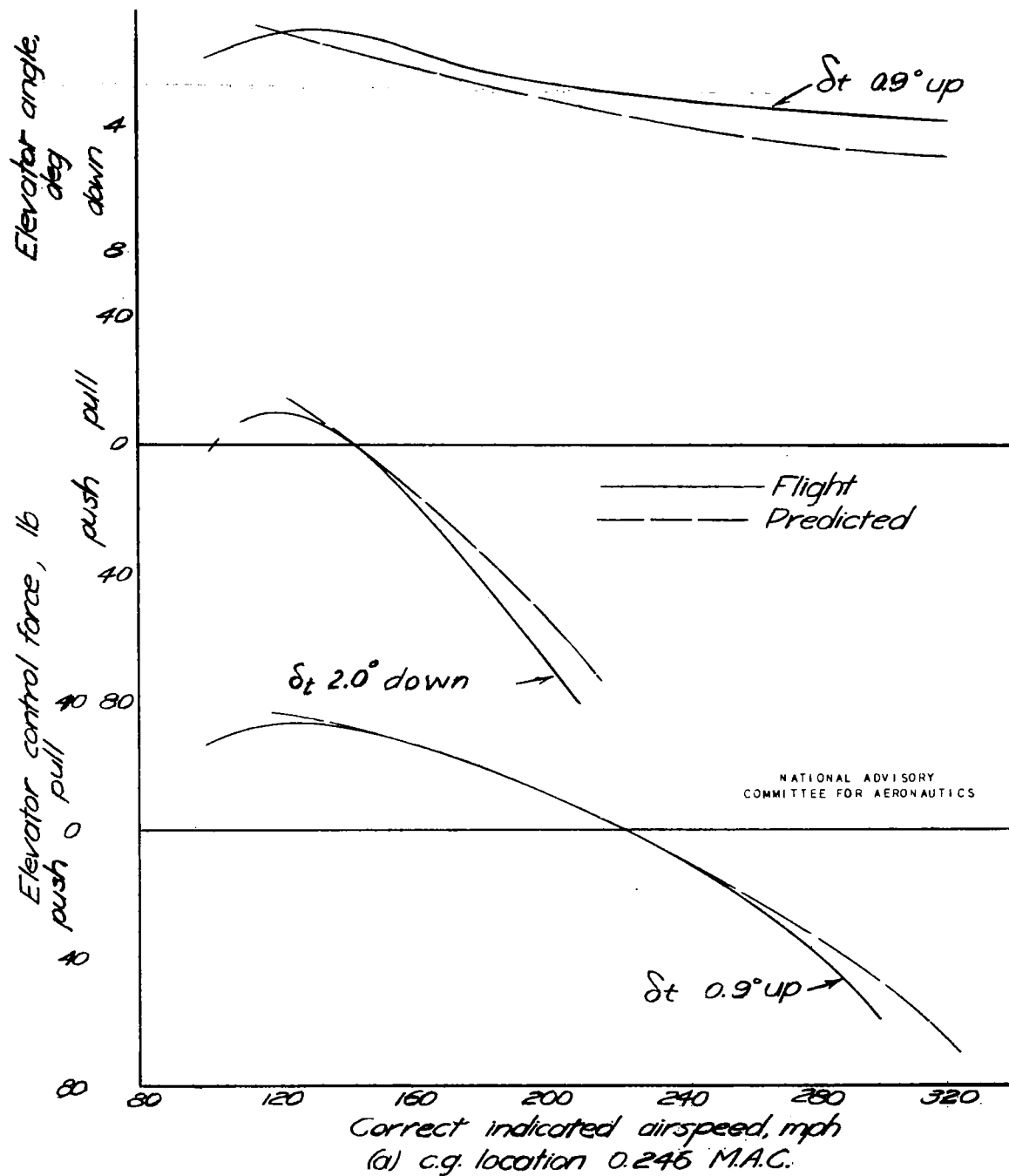
Figure 15.— Variation of elevator angle and control force with airspeed, climb condition. Steady straight unyawed flight.
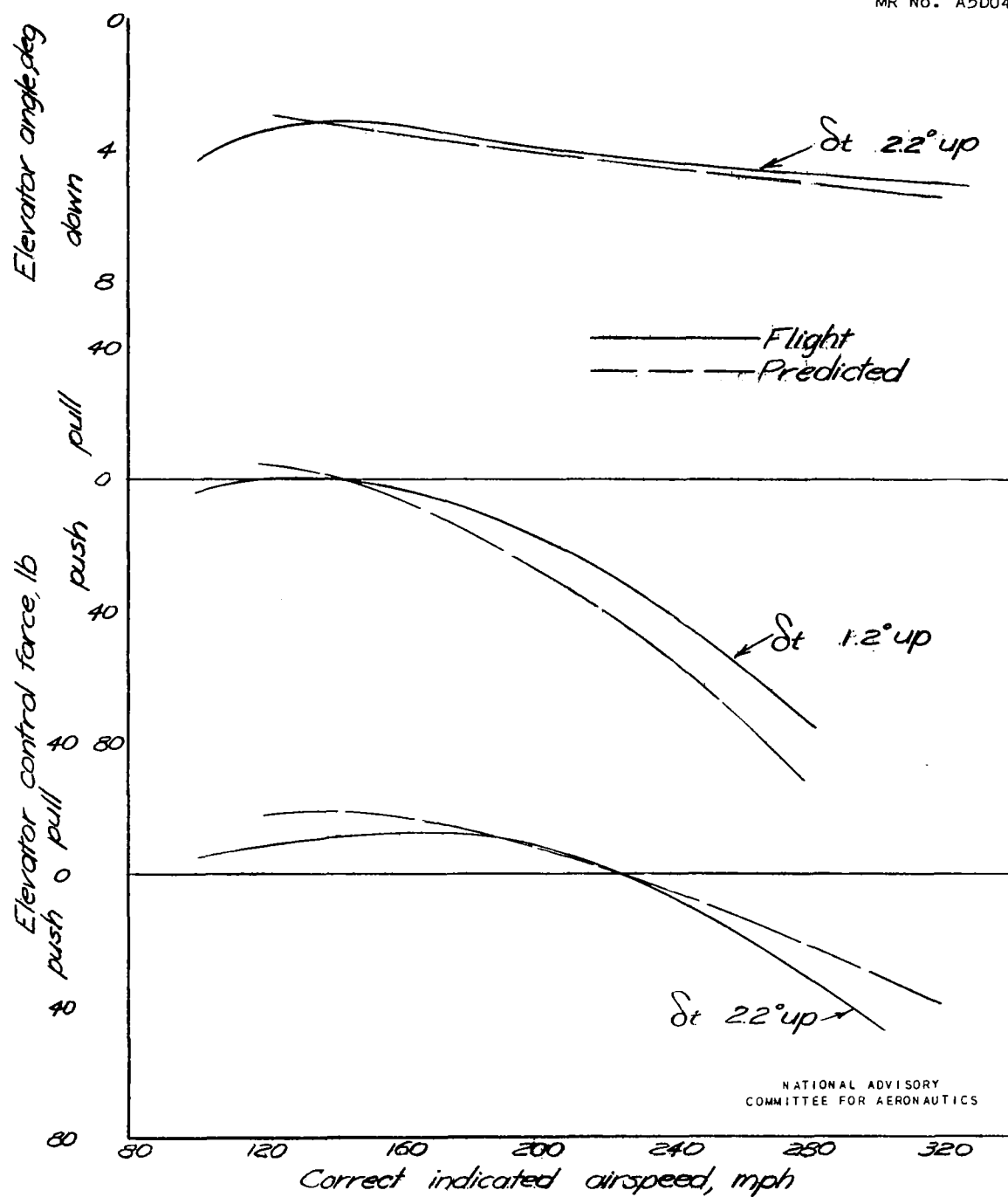
(b) c.g. location 0.272 M.A.C.

Figure 15 .- Climb condition, continued.
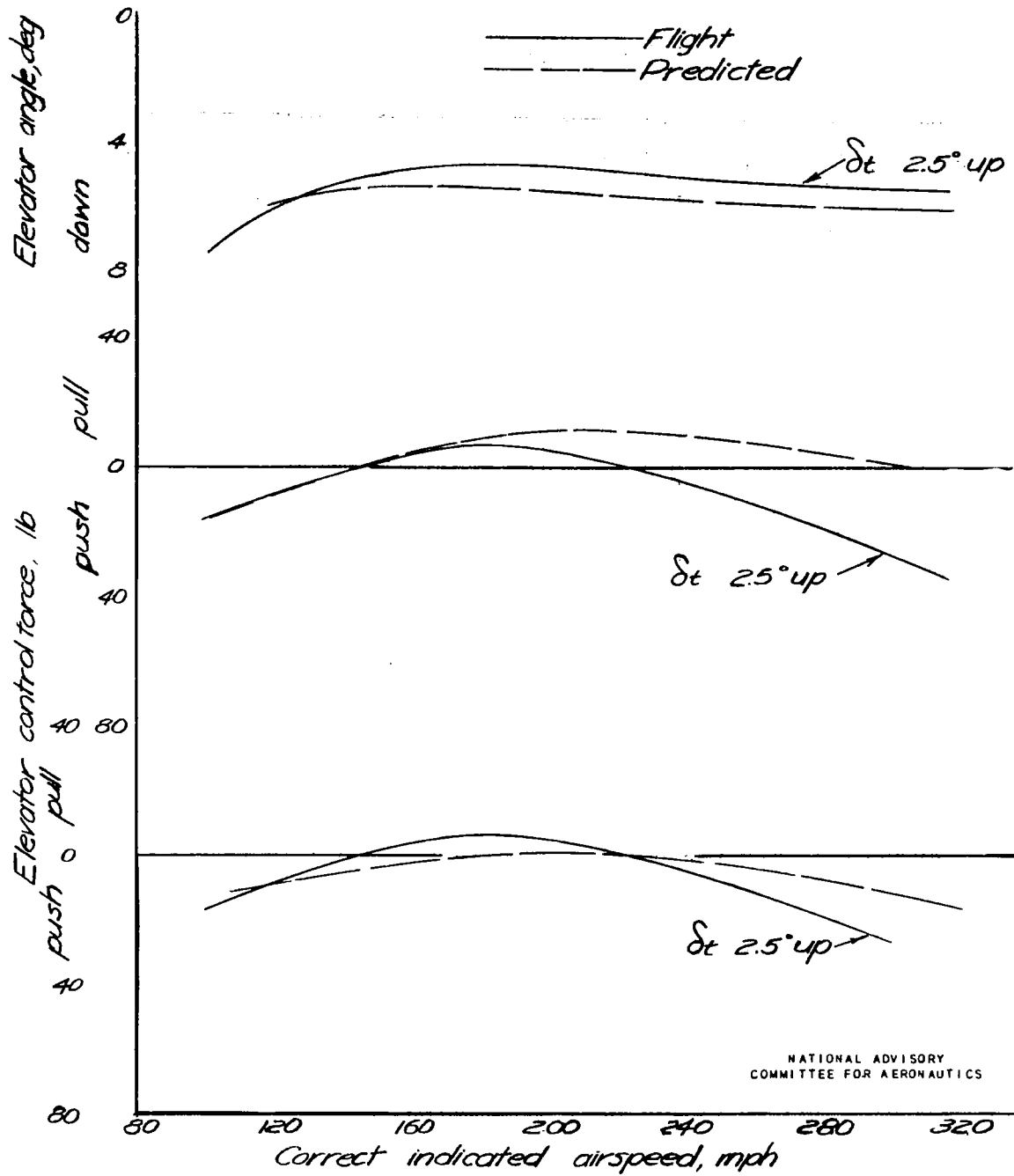
Figure 15 — Climb condition, concluded

(c) c.g. location 0.324 M.A.C.
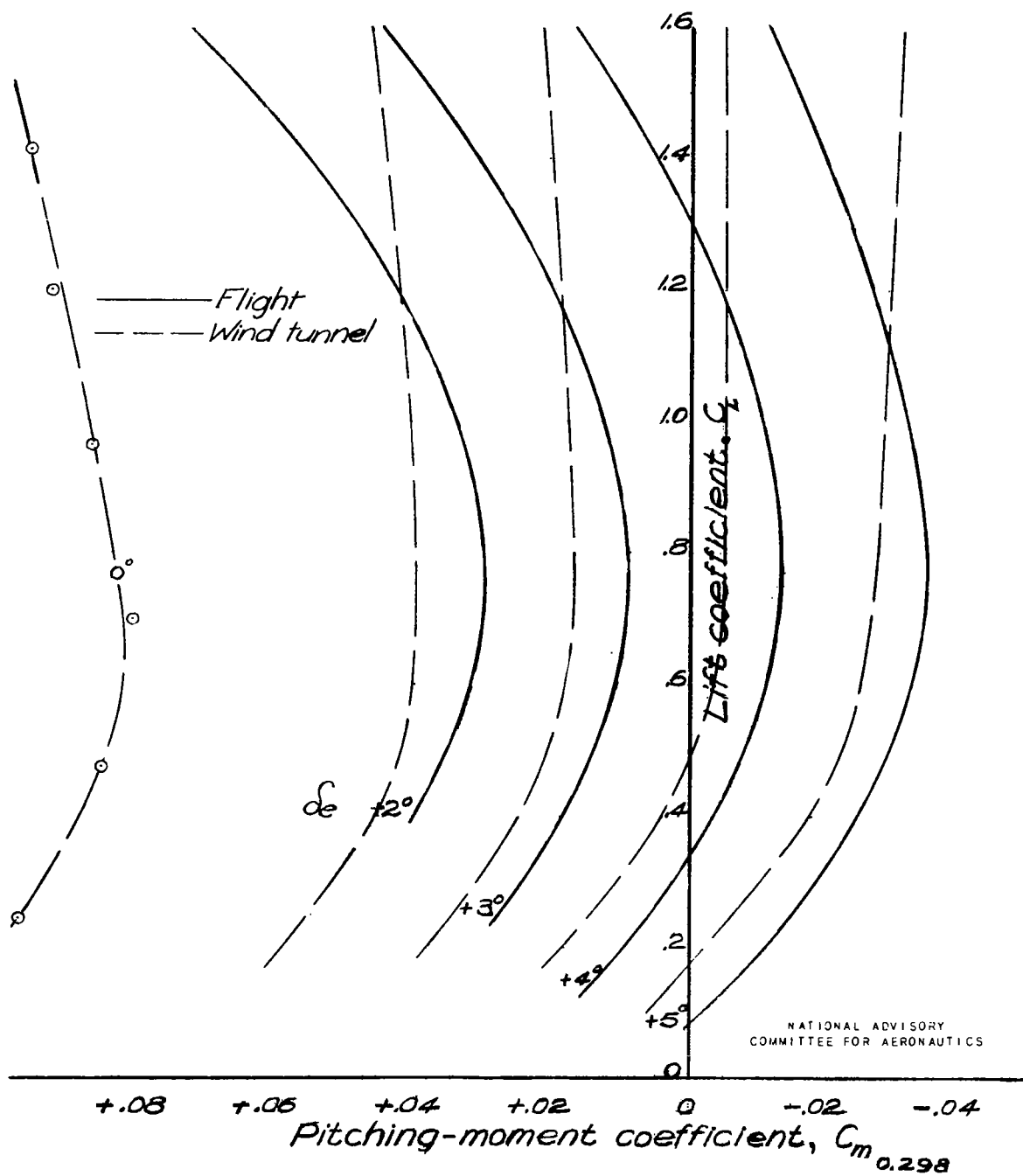
Figure 16.— Pitching-moment characteristics. Climb
condition.
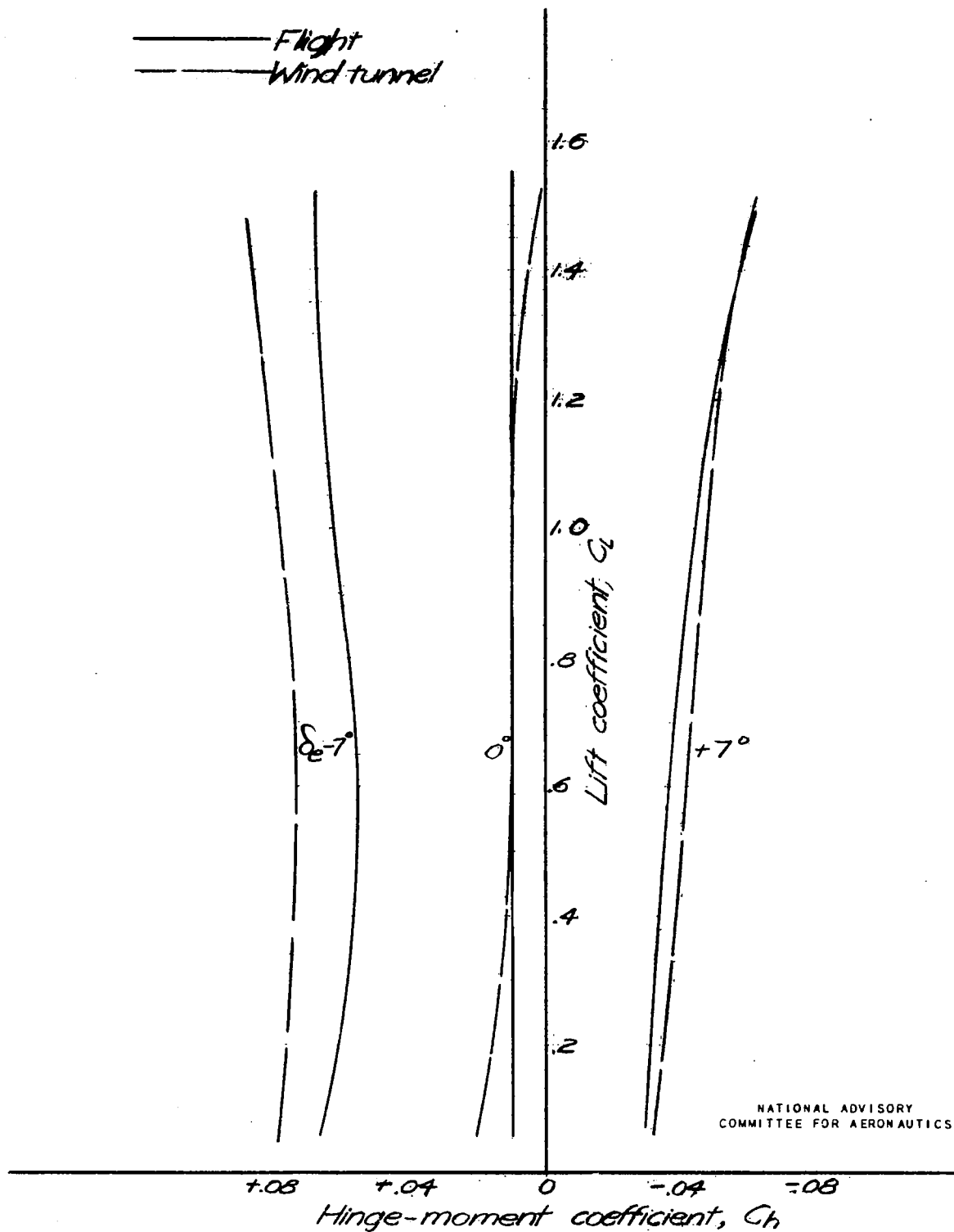
Figure 17.— Elevator hinge-moment characteristics. Climb condition

δt 15° down

Flight
Predicted

δt 15° down

NATIONAL ADVISORY
COMMITTEE FOR AERONAUTICS
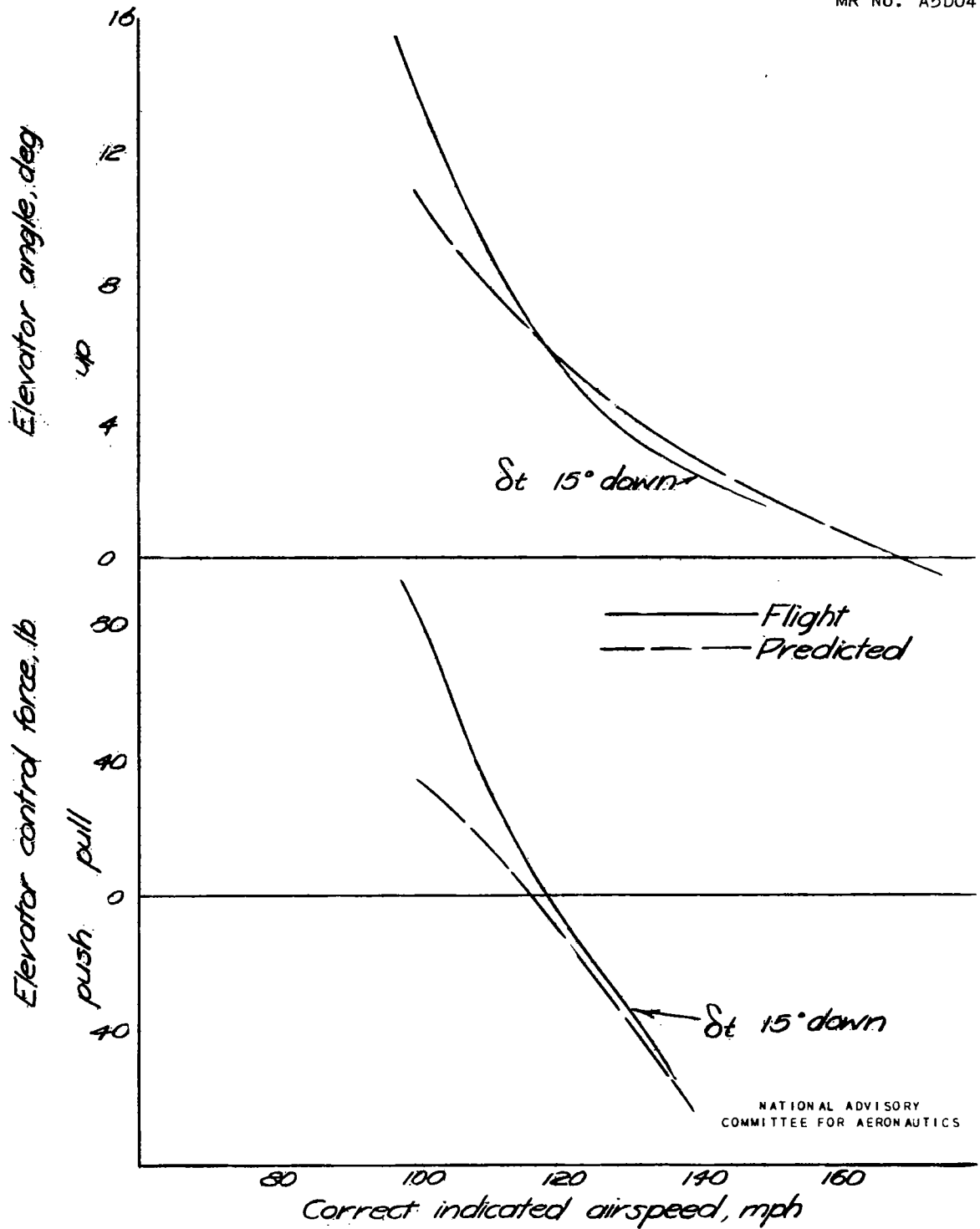
(a) c.g. location 0.229 M.A.C.

Figure 18 .—Variation of elevator angle and control force with airspeed, landing condition. Steady straight unyawed flight.
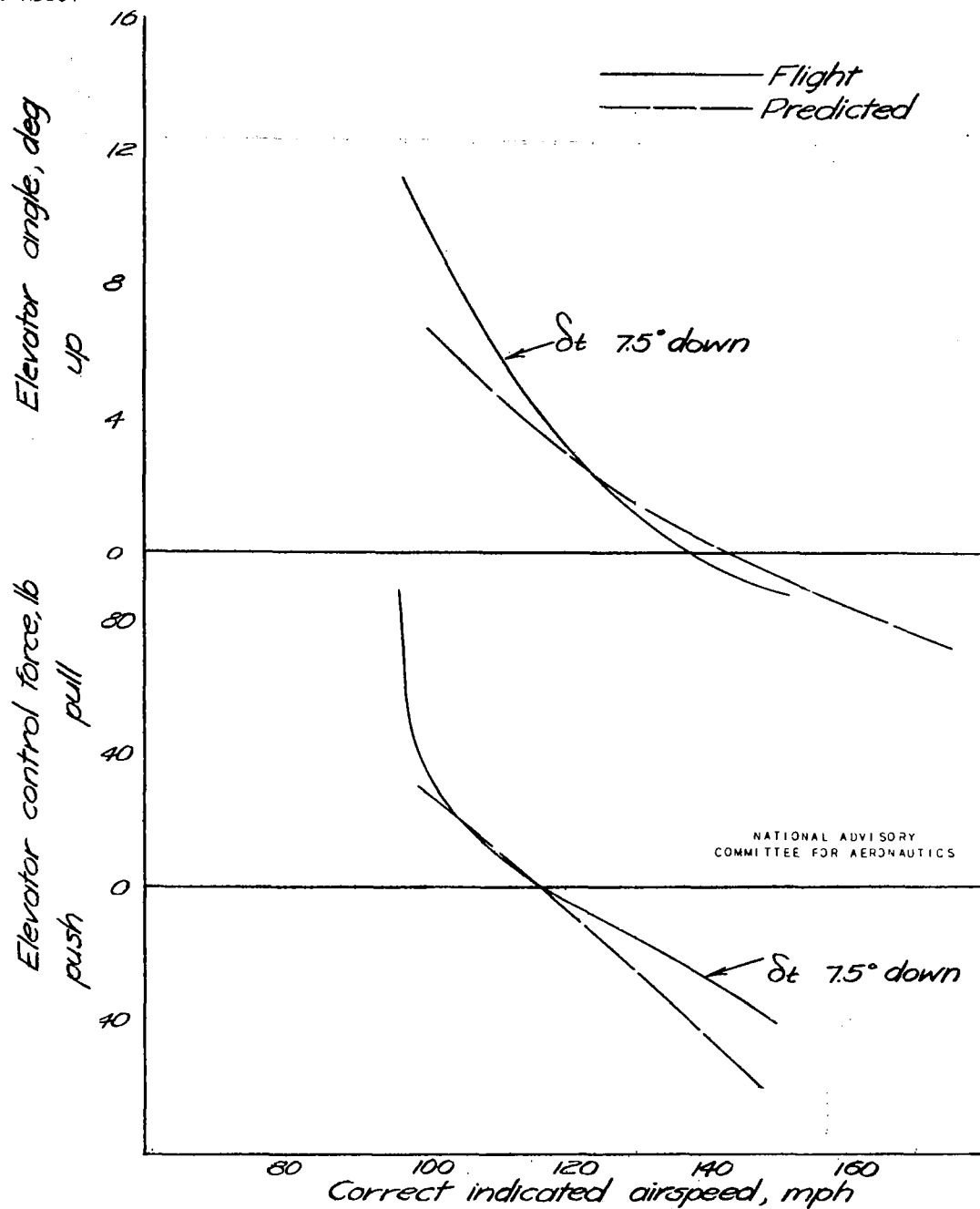
Figure 18 .- Landing condition, continued.

(b) c.g. location 0.265 M.A.C.

Correct indicated airspeed, mph
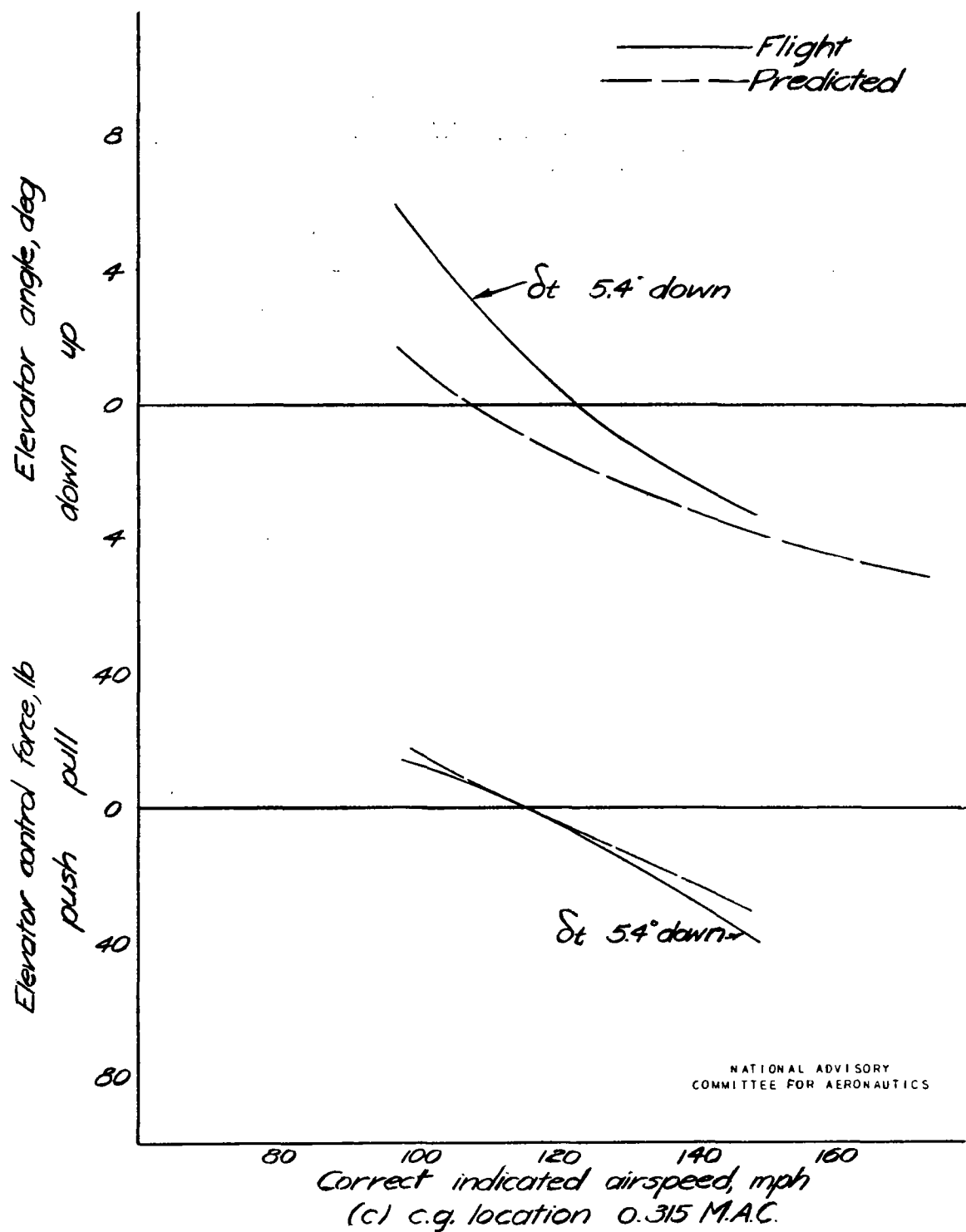
Figure 18 .- Landing condition, concluded.

(c) c.g. location 0.315 M.A.C.

Correct indicated airspeed, mph

Figure 19.— Pitching-moment characteristics. Landing condition.
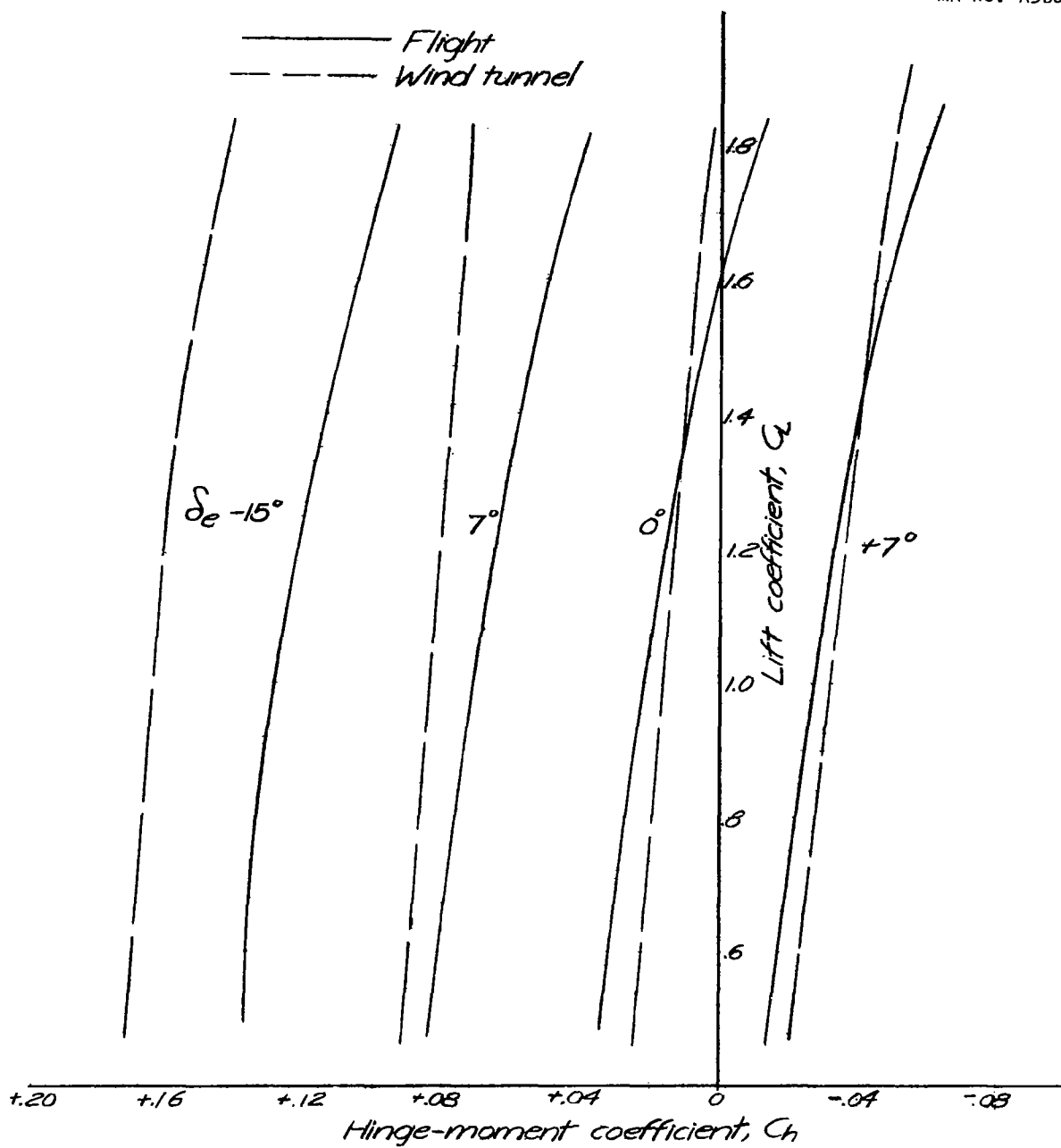
Figure 20 — Elevator hinge-moment characteristics. Landing condition.
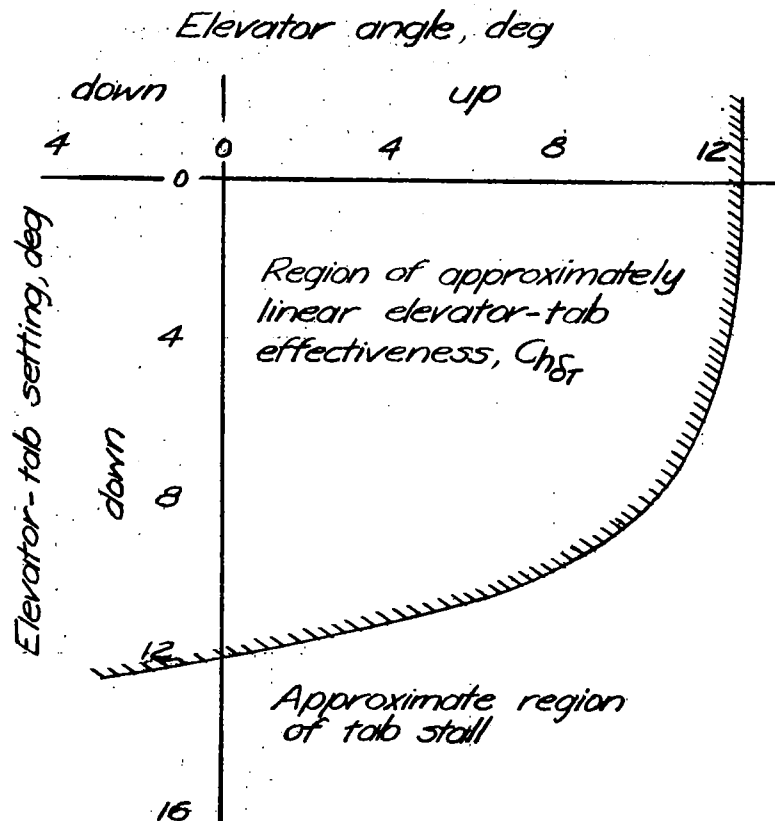
Figure 21 — Variation with elevator angle of the maximum elevator-tab settings for linear effectiveness $C_{h_{\delta_T}}$, approach and landing conditions.

(a) c.g. location 0.229 M.A.C.

Figure 22 .— Variation of elevator angle and control force with airspeed, approach condition. Steady straight unyawed flight.
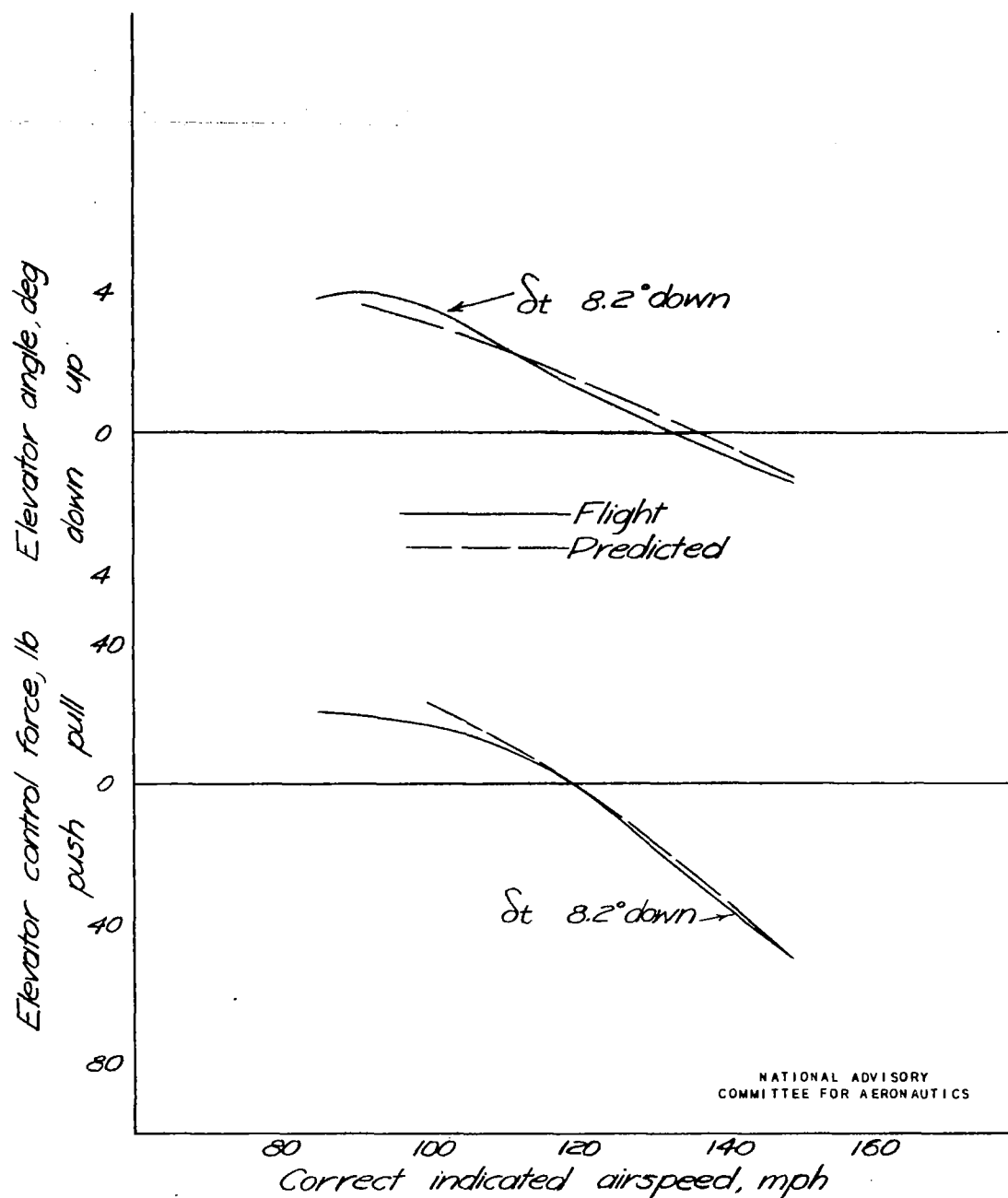
(b) c.g. location 0.267 M.A.C.

Figure 22 .- Approach condition, continued.
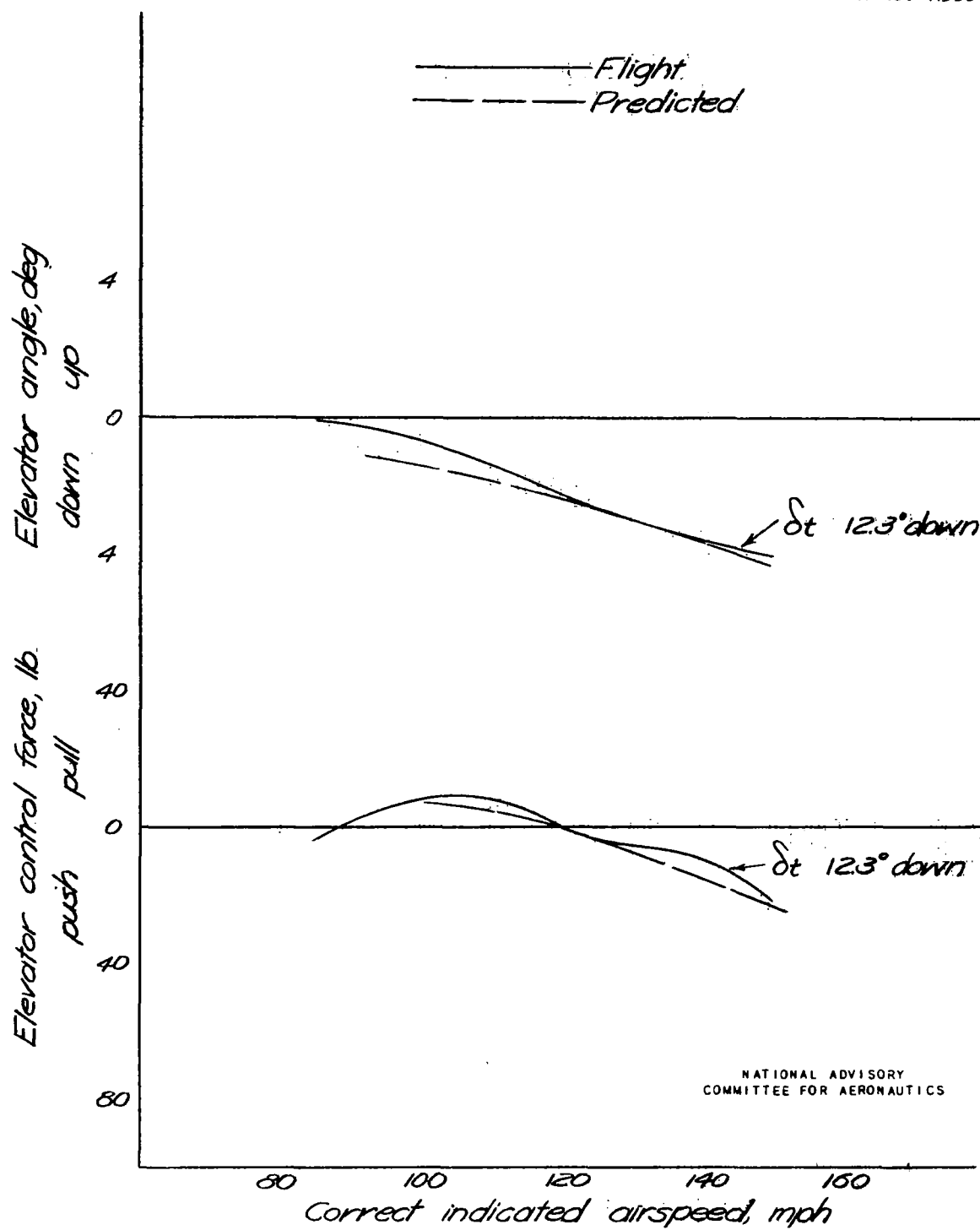
(c) c.g. location 0.314 M.A.C.

Figure 22 .— Approach condition, concluded.
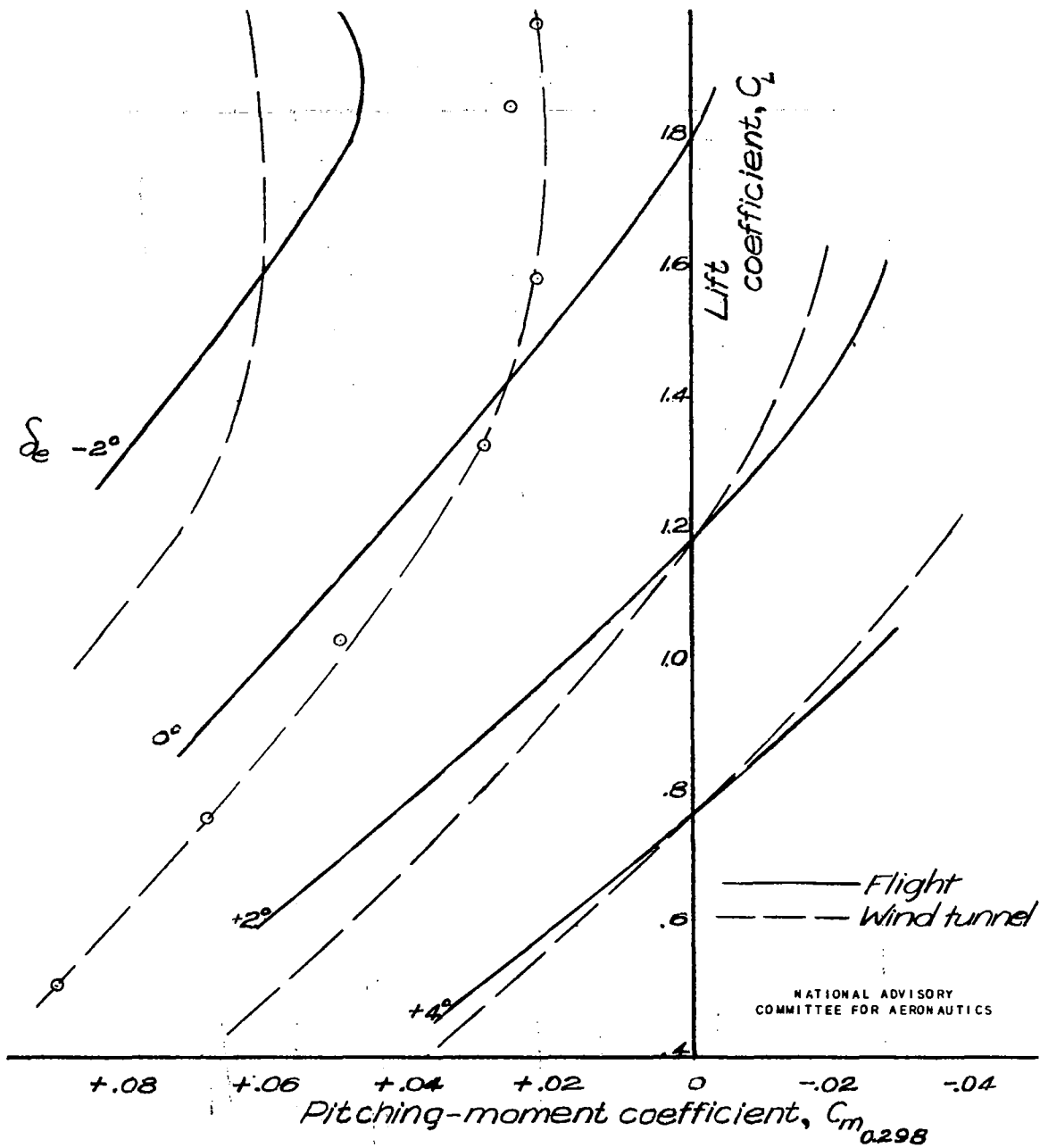
Figure 23.— Pitching-moment characteristics. Approach condition.
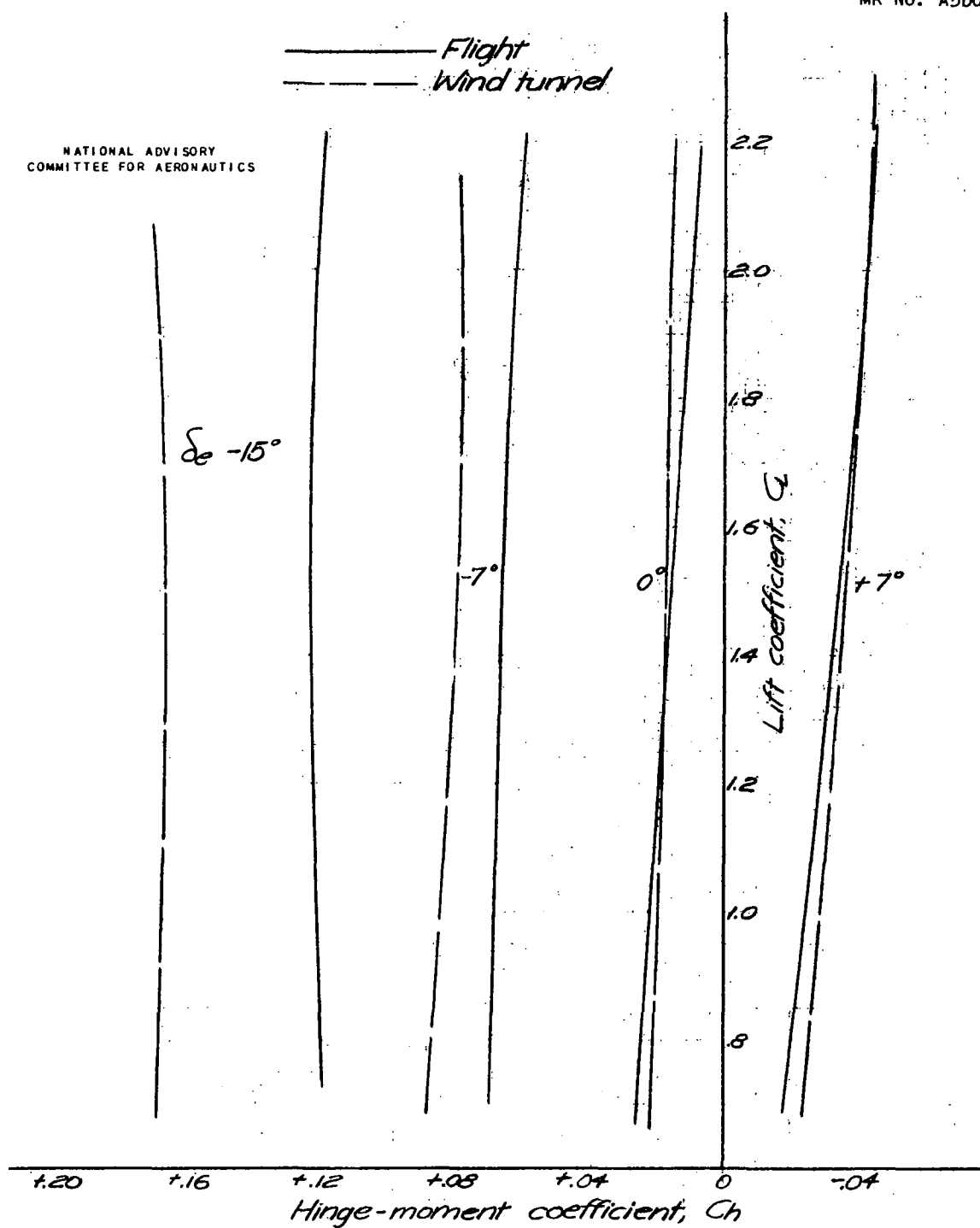
Figure 24.- Elevator hinge-moment characteristics
Approach condition
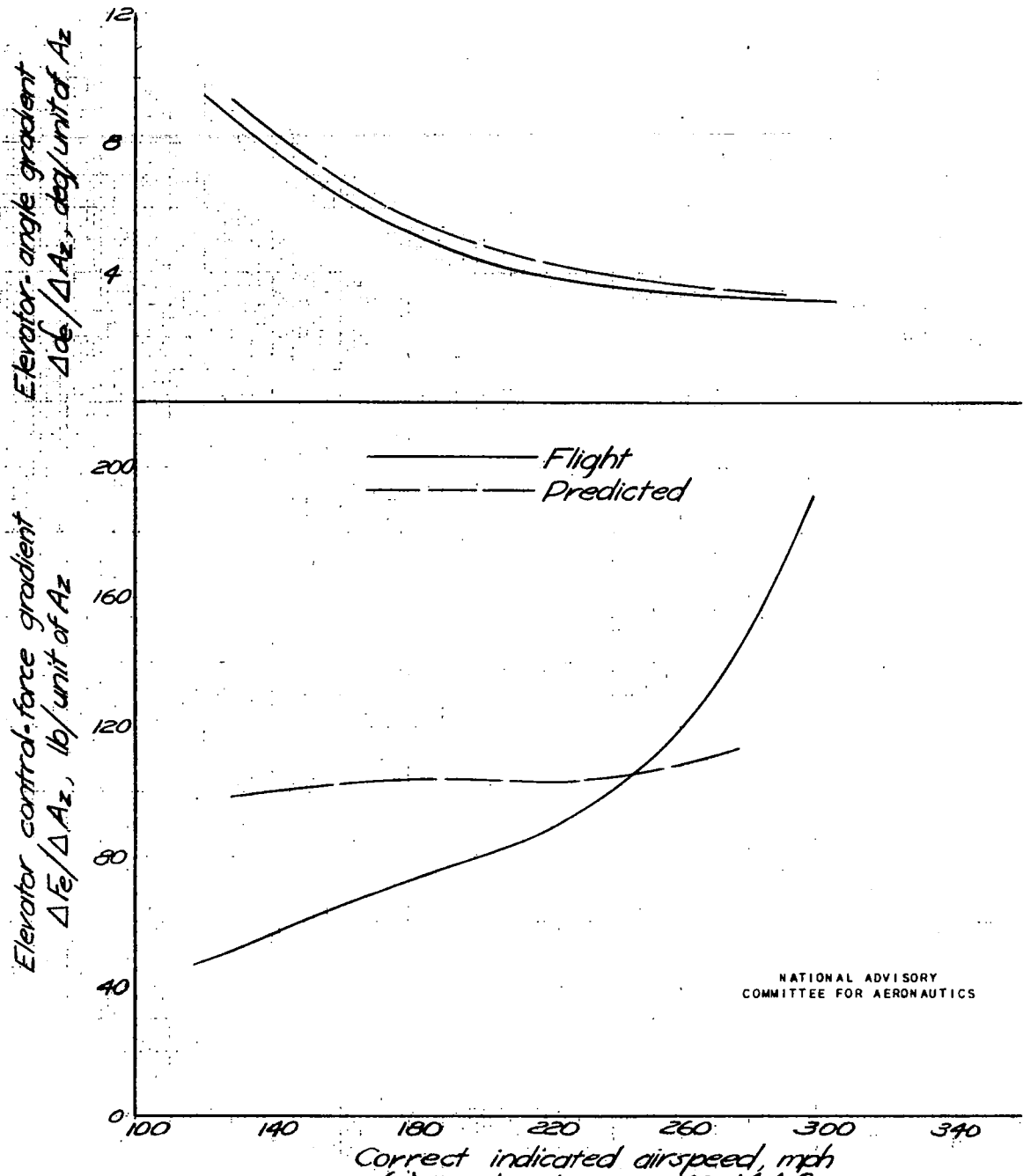
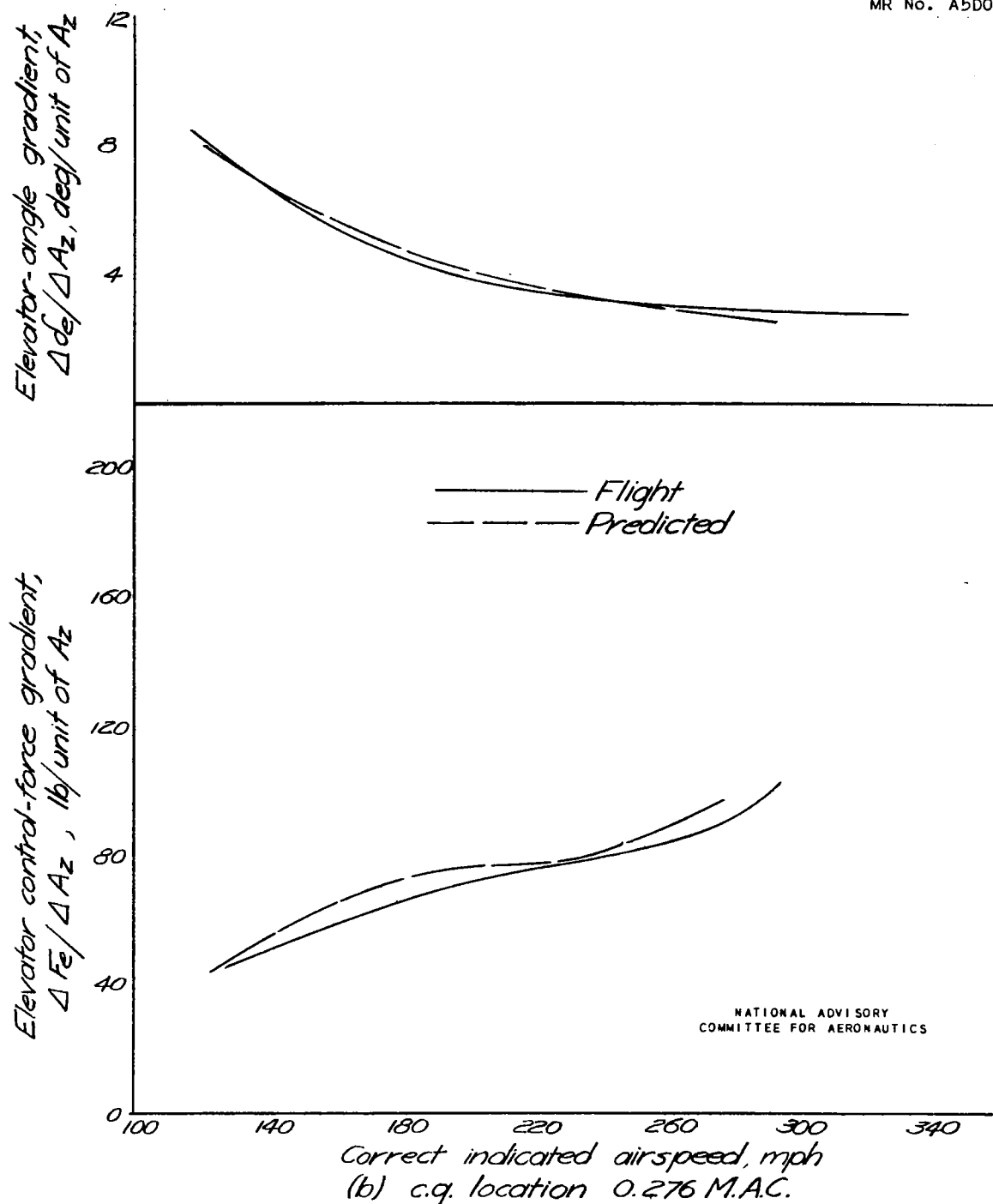Figure 25 .- Elevator-angle and control-force gradients in steady turns, climb condition.

Elevator-angle gradient, $\Delta \delta_e / \Delta A_z$, deg/unit of A_z

Elevator control-force gradient, $\Delta F_e / \Delta A_z$, lb/unit of A_z

——————— Flight
— — — — — Predicted

Correct indicated airspeed, mph

(b) c.g. location 0.276 M.A.C.

Figure 25 .— Continued.

MR No. A5D04

(c) c.g. location 0.324 M.A.C.
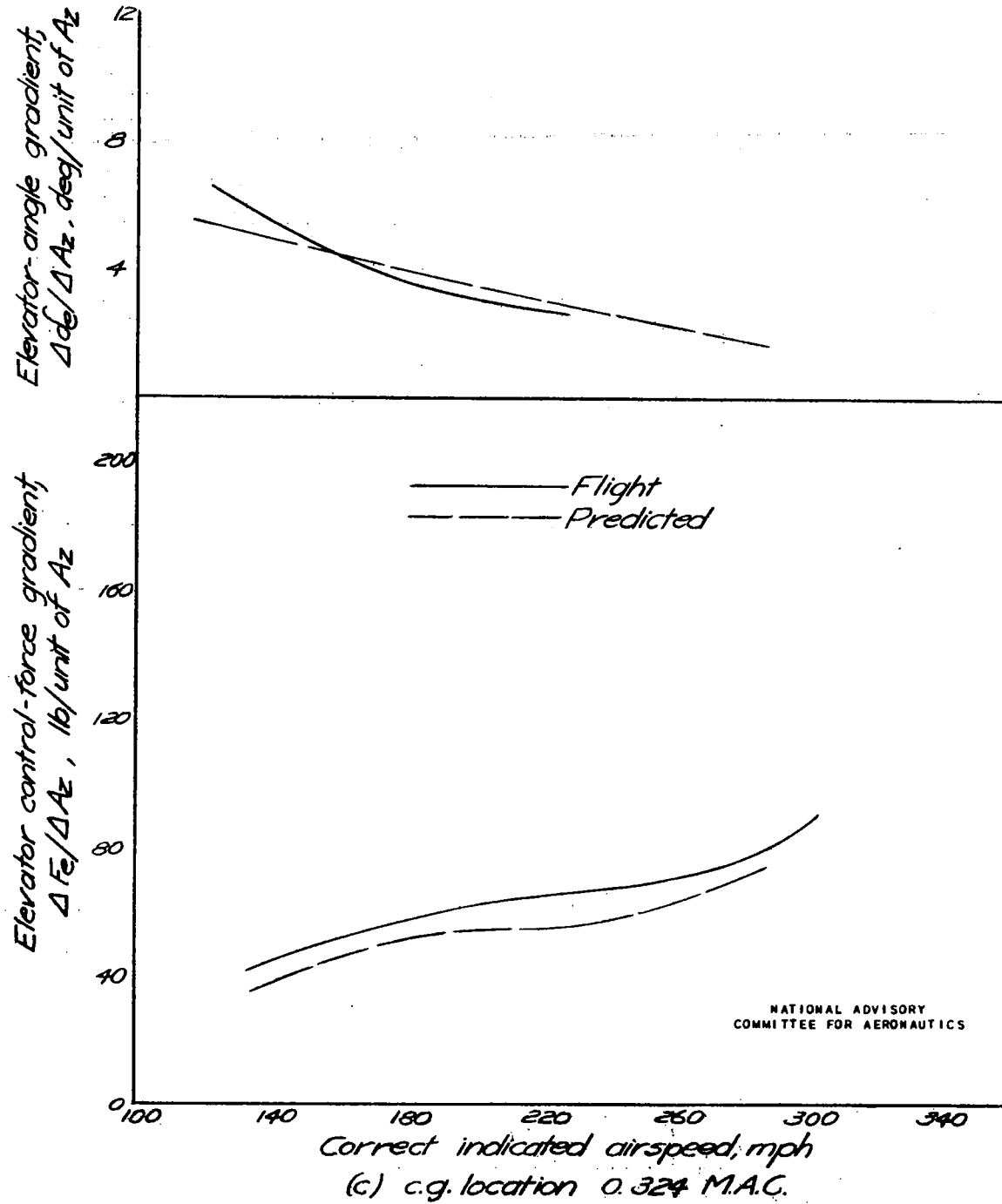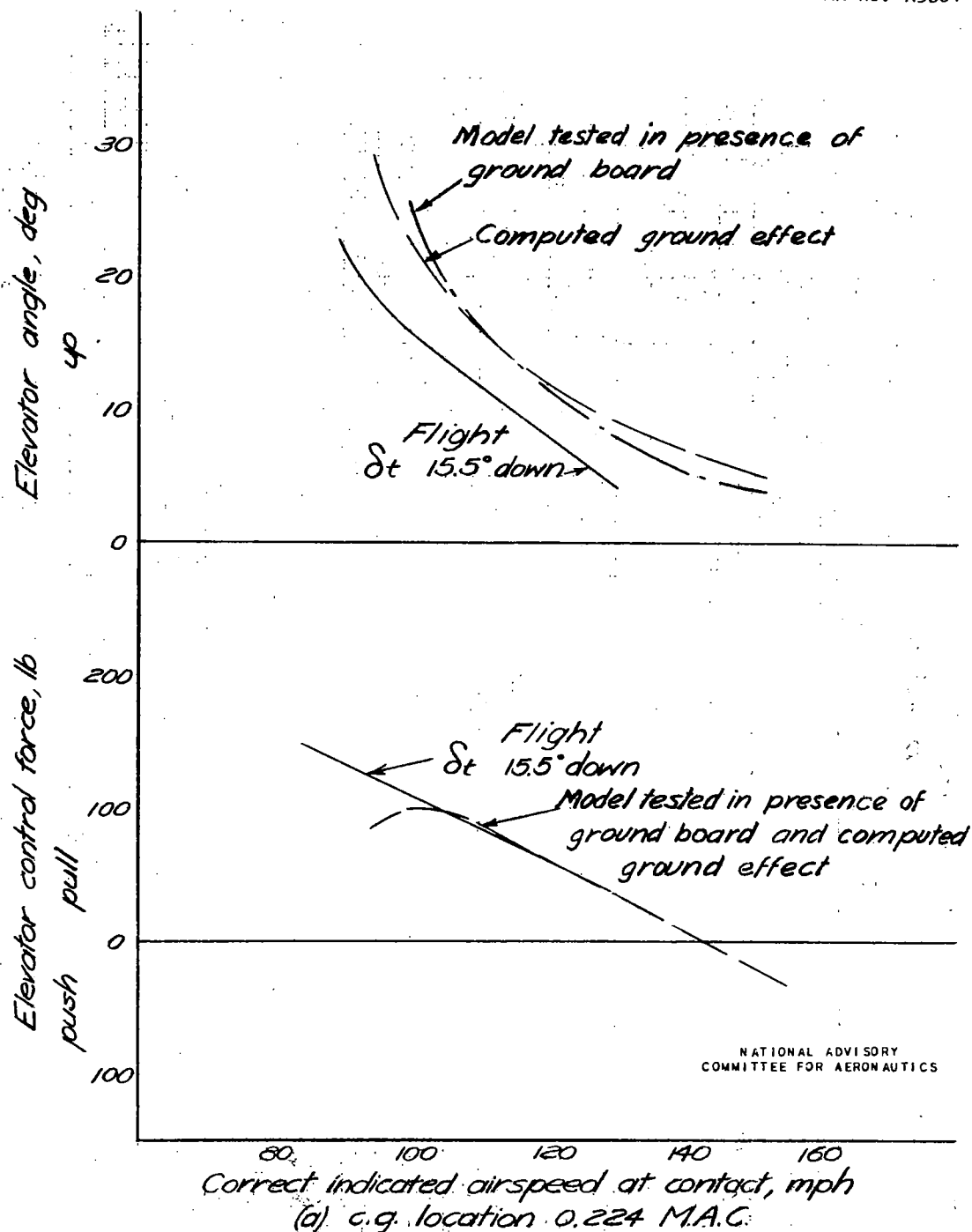
Figure 25 .- Concluded.

Figure 26 — Variation of elevator angle and control force with contact airspeed in landings.
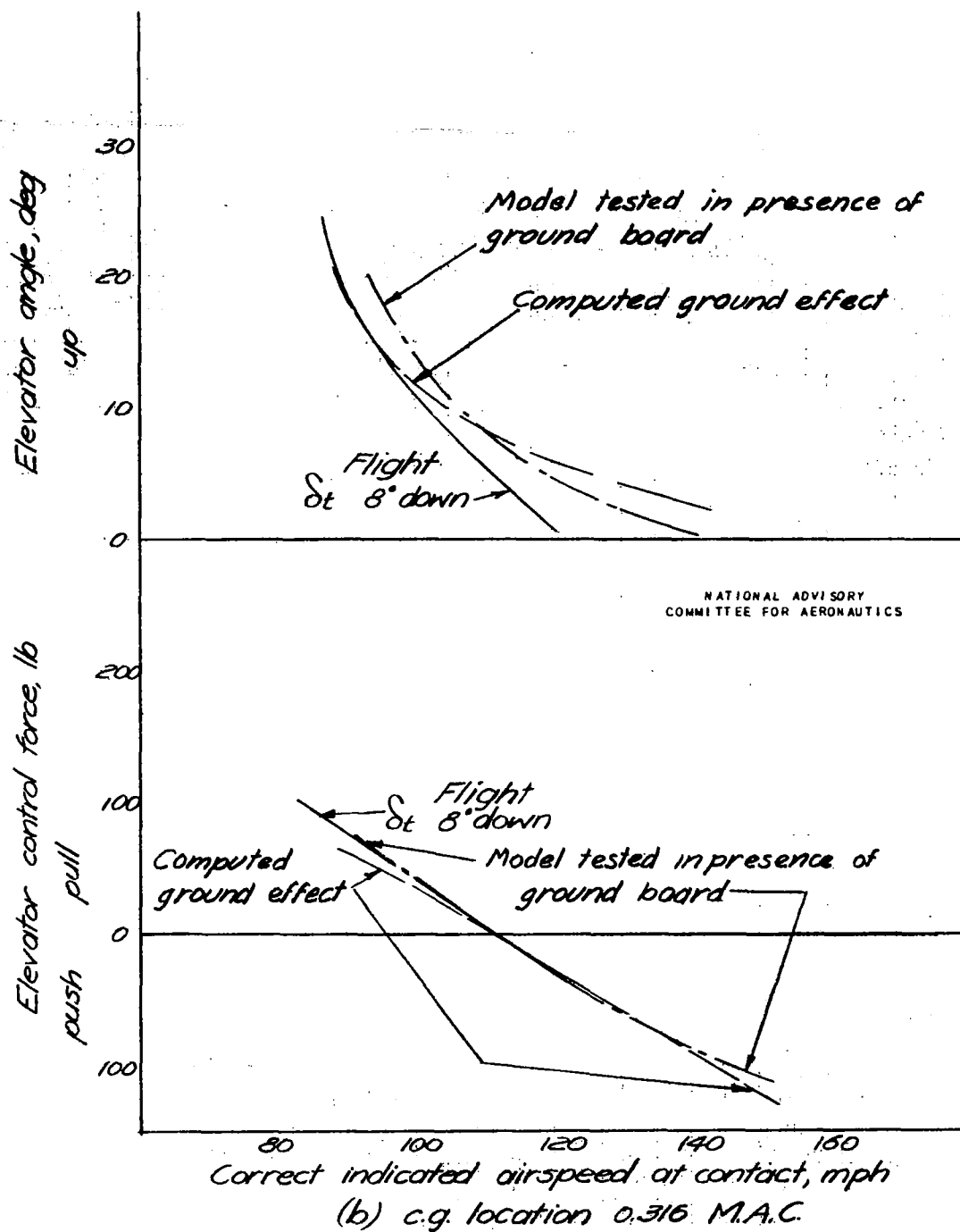
Figure. 26 .— Landings, concluded.